

Review

A Review on Predicting Ground PM_{2.5} Concentration Using Satellite Aerosol Optical Depth

Yuanyuan Chu ^{1,2,†}, Yisi Liu ^{1,†}, Xiangyu Li ^{1,2}, Zhiyong Liu ³, Hanson Lu ⁴, Yuanan Lu ^{2,5}, Zongfu Mao ^{1,2}, Xi Chen ¹, Na Li ¹, Meng Ren ¹, Feifei Liu ¹, Liqiao Tian ⁶, Zhongmin Zhu ^{6,7} and Hao Xiang ^{1,2,*}

- ¹ Department of Epidemiology and Biostatistics, School of Public Health, Wuhan University, 115# Donghu Road, Wuhan 430071, China; 2014203050033@whu.edu.cn (Y.C.); roselewis@sina.com (Y.L.); 2015203050022@whu.edu.cn (X.L.); zfmiao@126.com (Z.M.); aries_c_7@163.com (X.C.); 2012302170047@whu.edu.cn (N.L.); melodyrren@163.com (M.R.); 2015203050008@whu.edu.cn (F.L.)
 - ² Global Health Institute, Wuhan University, 115# Donghu Road, Wuhan 430071, China; yuanan@hawaii.edu
 - ³ The National Environmental Satellite, Data, and Information Service (NESDIS), National Oceanic and Atmospheric Administration (NOAA), 5830 University Research Court, College Park, MD 20740, USA; Zhiyonglau@gmail.com
 - ⁴ International Baccalaureate Diploma Program, Wuhan Foreign Languages School, Wan Song Yuan Road, Wuhan 430022, China; hansonlu_hl@hotmail.com
 - ⁵ Environmental Health Laboratory, Department of Public Health Sciences, University of Hawaii at Manoa, 1960 East-West Road, Honolulu, HI 96822, USA
 - ⁶ State Key Laboratory of Information Engineering in Surveying, Mapping and Remote Sensing, Wuhan University, 129# Luoyu Road, Wuhan 430079, China; tianliqiao@whu.edu.cn (L.T.); zhongmin.zhu@whu.edu.cn (Z.Z.)
 - ⁷ College of Information Science and Engineering, Wuchang Shouyi University, Wuhan 430064, China
- * Correspondence: xianghao@whu.edu.cn; Tel.: +86-27-6875-9118
† These authors contributed equally to this work.

Academic Editor: Robert W. Talbot

Received: 25 July 2016; Accepted: 5 October 2016; Published: 14 October 2016

Abstract: This study reviewed the prediction of fine particulate matter (PM_{2.5}) from satellite aerosol optical depth (AOD) and summarized the advantages and limitations of these predicting models. A total of 116 articles were included from 1436 records retrieved. The number of such studies has been increasing since 2003. Among these studies, four predicting models were widely used: Multiple Linear Regression (MLR) (25 articles), Mixed-Effect Model (MEM) (23 articles), Chemical Transport Model (CTM) (16 articles) and Geographically Weighted Regression (GWR) (10 articles). We found that there is no so-called best model among them and each has both advantages and limitations. Regarding the prediction accuracy, MEM performs the best, while MLR performs worst. CTM predicts PM_{2.5} better on a global scale, while GWR tends to perform well on a regional level. Moreover, prediction performance can be significantly improved by combining meteorological variables with land use factors of each region, instead of only considering meteorological variables. In addition, MEM has advantages in dealing with the AOD data with missing values. We recommend that with the help of higher resolution AOD data, future works could be focused on developing satellite-based predicting models for the prediction of historical PM_{2.5} and other air pollutants.

Keywords: aerosol optical depth; PM_{2.5}; satellite retrieving; Mixed-Effect Model; Chemical Transport Model

1. Introduction

According to the World Health Organization's report in 2014, 3.7 million premature deaths related to ambient air pollution occurred around the world in 2012 [1]. Ambient air pollutants include particulate matter, ozone, nitrogen dioxide, sulfur dioxide, and other contaminants. Fine particulate matter with aerodynamic diameters smaller than $2.5 \mu\text{m}$ ($\text{PM}_{2.5}$) is the most problematic of these pollutants. $\text{PM}_{2.5}$ particles can enter into the alveoli, subsequently being retained in the lung parenchyma [2]. Due to the toxicological effects of the resulting inflammation and oxidative stress [3], $\text{PM}_{2.5}$ can cause severe cardiovascular diseases, respiratory diseases and even lung cancer [4,5]. A study of the global burden of disease study in 1990–2010 ranked ambient $\text{PM}_{2.5}$ concentrations ninth out of all health risk factors [6]. $\text{PM}_{2.5}$ has therefore played an important role in the area of air pollution and environmental health [7–10].

However, most pollutant concentration information was obtained from ground monitoring stations, which have many limitations. These stations are limited in number, unequally distributed [7,11] and have different measure frequency ranges [12]. These limitations may affect the geographical and demographical range of studies, resulting in an information bias and reducing the confidence in the results of exposure response studies [13]. Furthermore, the temporal and spatial variation of $\text{PM}_{2.5}$ is complex, and continuous monitoring of $\text{PM}_{2.5}$ is absent in many countries and regions [14]. For example, $\text{PM}_{2.5}$ was not included in China's national monitoring system until 2013. Remote sensing techniques could therefore allow the collection of long period continuous $\text{PM}_{2.5}$ data on large spatial scales over China [15].

Numerous researchers have attempted to estimate ground $\text{PM}_{2.5}$ levels using satellite-derived atmospheric aerosol optical depth (AOD) [16], which is the aerosol extinction coefficient of accumulated points in the vertical direction [4,16,17]. Satellite-derived AOD research began in the mid-1970s, and, in 2003, Wang et al. [16] initiated the use of Moderate Resolution Imaging Spectrometer (MODIS) AOD in the prediction for ground level $\text{PM}_{2.5}$ through linear correlation. Liu et al. [18] came up with Chemical Transport Model (CTM) in 2004, and, in 2011, Lee et al. [19] created the day-specific Mixed-Effect Model (MEM) using MODIS AOD. In recent years, $\text{PM}_{2.5}$ levels have been estimated using a variety of satellite sensors, including the MODIS [20,21], the Multi-Angle Imaging Spectrometer (MISR) [4,20,22], the Geostationary Operational Environment Satellite (GEOS) [23,24], Polarization of Earth's Reflectance and Directionality (POLDER) [25,26], the Sea-viewing Wide Field-of-view Sensor (SeaWiFS) [27,28], the Ozone Monitoring Instrument (OMI) [29] and the Cloud-Aerosol Lidar with Orthogonal Polarization (CALIOP) [29,30]. Although studies of this kind are becoming more common, prediction results have been unstable and varied significantly between different regions [31,32]. Additionally, different studies have used different methods of dealing with missing AOD data [7,33–36]. The objective of this study is to review previous studies in order to compare existing $\text{PM}_{2.5}$ predicting models based on satellite AOD and illustrate their advantages and limitations. This could provide a helpful reference for future satellite-based $\text{PM}_{2.5}$ predicting studies.

2. Methods

2.1. Subject of This Review

What is the relationship between $\text{PM}_{2.5}$ concentrations predicted from aerosol optical depth retrieval and $\text{PM}_{2.5}$ concentrations measured on the ground?

2.2. Search Criteria

We searched the following electronic databases prior to 30 June 2016: Web of Science (WOS), PubMed, Engineering Index (EI), Nature, Elsevier Science Direct, Wiley, Springer, and Taylor and Francis. Keywords used in the searches included: aerosol optical depth (AOD, aerosol optical thickness, AOT), fine particulate matter ($\text{PM}_{2.5}$), satellite data, satellite remote sensing, satellite derived, and satellite retrieved. These keywords were searched under the categories of "subject",

“title”, and “keywords” respectively, connected through logical combinations of “and” and “or”. When searching in Web of Science, for example, we used the following combination of keywords: (“aerosol optical depth”) OR (“AOD”) OR (“aerosol optical thickness”) OR (“AOT”) OR (“satellite data”) OR (“satellite remote sensing”) OR (“satellite derived”) OR (“satellite retrieved”) AND (“fine particulate matter”) OR (“PM_{2.5}”).

2.3. Inclusion and Exclusion Criteria

The inclusion criteria are as follows: (1) papers published in the peer-reviewed journals before 30 June 2016; (2) empirical research utilizing both satellite AOD data and ground PM_{2.5} data; and (3) papers incorporating PM_{2.5} predicting models based on satellite-derived AOD and model evaluation. During the process of abstract and full texts reviewing, studies were excluded according to these criteria: (1) abstracts and conferences only; (2) studies using AOD data only or PM_{2.5} data only, and studies without R² values; and (3) satellite-based PM_{2.5} predicting studies conducted over the ocean or special terrains (such as mountains), or during the following natural and anthropogenic events: land (forest) fires, dust storms, volcanic eruptions, and fuel combustion events. We reviewed all the selected studies in detail and summarized their main features.

3. Results

After screening 1436 identified studies and assessing the eligibility of the remaining studies, we selected 116 articles for our review that are primarily relevant to the satellite-based PM_{2.5} predicting model (Figure 1). The study areas, results, models used and other basic characteristics of all included studies are summarized in Table 1.

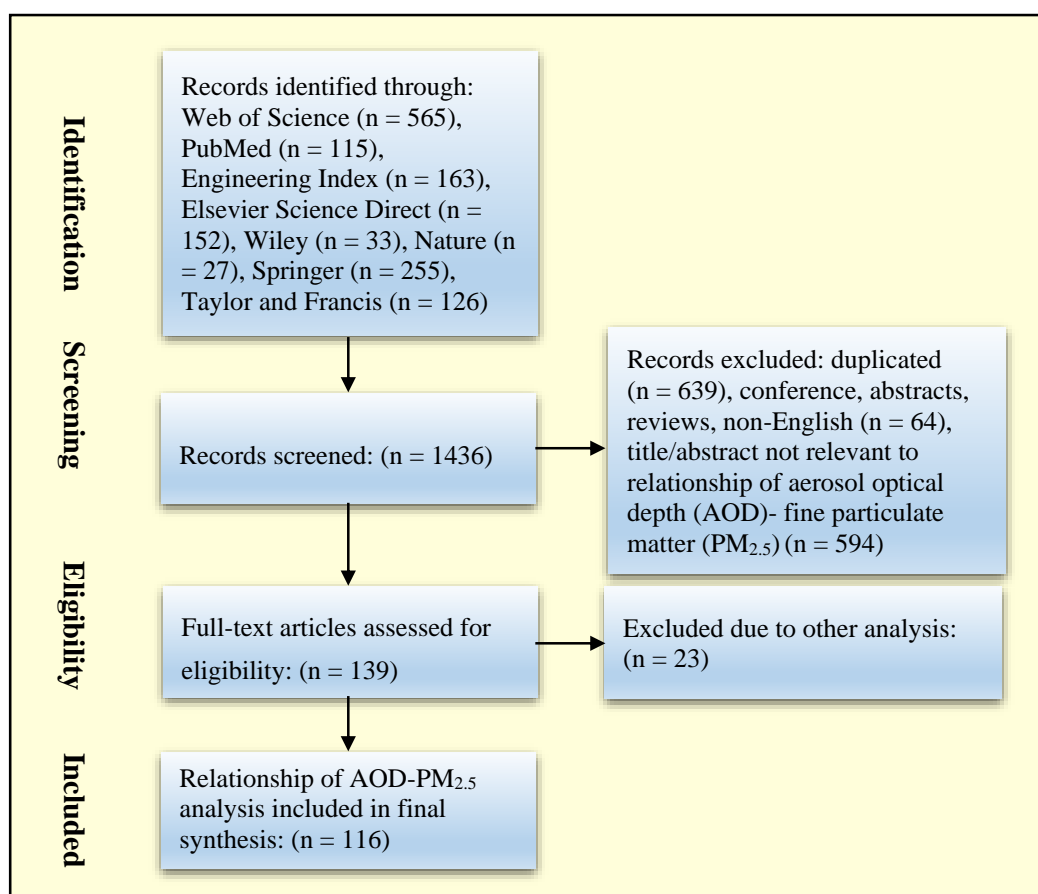


Figure 1. Flow chart of study selection.

Table 1. Characteristics of included studies.

Author (Published Year)	Study Area	Study Period	Source of AOD	Retrieved Model	R ² of Model (CV-R ²)
Wang et al. (2003) [16]	U.S.	2002	MODIS	LC	0.960 ^a (N ^{ss} = 1, N ^{ms} = 7)
Engel-Cox et al. (2004) [31]	U.S.	2002	MODIS	LC	0.185 ^{a,b}
Liu et al. (2004) [18]	U.S.	2001	MISR	CTM	0.656 ^{a,b} (Yearly, N ^{ms} = 1268)
Hutchison et al. (2005) [37]	U.S.	2003–2004	MODIS	LC	0.160–0.250 ^{a,b} (N ^{ms} = 51)
Liu et al. (2005) [38]	U.S.	2001	MISR	MLR	0.430 ^{a,b} (N ^{ms} = 346)
Chu et al. (2006) [39]	U.S.	2002	MODIS	MLR	0.723 ^a (New York), 0.757 ^a (Chicago), 0.774 ^a (Houston) (N ^{ms} = 350 for U.S.)
Engel-Cox et al. (2006) [40]	U.S.	2004	MODIS	MLR	0.423 ^a
Gupta et al. (2006) [41]	Global	2000–2002	MODIS	MLR	0.960 ^{a,b} (N ^{ss} = 26, N ^{ms} = 113)
Kacenenlobogen et al. (2006) [26]	France	2003	POLDER	MLR	0.490 ^{a,b} (when the matched data is 78), 0.310 ^{a,b} (N ^{ms} = 28, when the matched data is 1974)
Koelemeijer et al. (2006) [42]	Europe	2003	MODIS	LC	0.360 ^{a,b} (N ^{ms} = 88)
van Donkelaar et al. (2006) [43]	Global	2000–2001	MODIS, MISR	CTM	0.476 ^{a,b} (MODIS, N ^{ms} = 199), 0.325 ^{a,b} (MISR, N ^{ms} = 199)
Kumar et al. (2007) [44]	India	2003	MODIS	MLR	0.700 ^{a,b} (Point/disaggregate-level analysis, N ^{ms} = 113), 0.610 ^{a,b} (Aggregate/pixel-level analysis, N ^{ms} = 113)
Liu et al. (2007) [13]	U.S.	2005	MISR	CTM	Eastern: 0.560 ^{a,b} (with fractional AOD, N ^{ms} = 130), 0.420 ^{a,b} (with total AOD, N ^{ms} = 130) Western: 0.570 ^{a,b} (with fractional AOD, N ^{ms} = 130), 0.210 ^{a,b} (with total AOD, N ^{ms} = 130)
Liu et al. (2007) [20]	U.S.	2003	MODIS, MISR	GLM	0.510 ^{a,b} (MODIS, St. Louis and its surrounding counties, N ^{ms} = 22), 0.620 ^{a,b} (MISR, St. Louis and its surrounding counties, N ^{ms} = 22)
Wallace et al. (2007) [45]	Canada	2015	MODIS	MLR	0.760 ^b (N ^{ms} = 34)
Gupta et al. (2008) [46]	U.S.	2000–2006	MODIS	MLR	0.520 ^{a,b} (Daily, N ^{ms} = 14), 0.620 ^{a,b} (Hourly, N ^{ms} = 14)
Gupta et al. (2008) [11]	U.S.	2000–2005	MODIS	MLR	0.270 ^{a,b} (N ^{ms} = 38)
Hutchison et al. (2008) [47]	U.S.	2003, 2004	MODIS	MLR	0.221 ^{a,b} (20 August–15 September, Hourly, Houston-Beaumont-Galveston area), 0.960 ^{a,b} (6–7 September, Hourly, Houston-Beaumont-Galveston area)
Kumar et al. (2008) [48]	India	2003	MODIS	MLR	0.700 ^{a,b} (Point/disaggregate-level analysis, Delhi and its environs, N ^{ms} = 113), 0.610 ^{a,b} (Aggregate/pixel-level analysis, Delhi and its environs, N ^{ms} = 113)
Paciorek et al. (2008) [24]	U.S.	2004	MODIS, MISR, GEOS	GAM	0.360 ^{a,b}

Table 1. Cont.

Author (Published Year)	Study Area	Study Period	Source of AOD	Retrieved Model	R ² of Model (CV-R ²)
Al-Hamdan et al. (2009) [49]	U.S.	2000–2003	MODIS	MLR	0.661–0.706 ^{a,b} (MODIS), 0.874 ^{a,b} (B-Spline, merged AQS/MODIS), 0.949 ^{a,b} (IDW, merged AQS/MODIS)
Green et al. (2009) [50]	U.S.	2003–2007	GEOS, MODIS	MLR	0.480 ^a (GEOS, N ^{ss} = 1), 0.740 ^a (MODIS, N ^{ss} = 1)
Gupta et al. (2009) [51]	U.S.	2004–2006	MODIS	MLR	0.365 ^{a,b} (TVM, N ^{ms} = 85), 0.466 ^{a,b} (MVM, N ^{ms} = 85)
Gupta et al. (2009) [52]	U.S.	2004–2006	MODIS	ANN	0.608 ^{a,b} (N ^{ms} = 85)
Hu et al. (2009) [32]	U.S.	2003–2004	MODIS	GWR, LC	0.449 ^{a,b} (LC, East), 0.048 ^{a,b} (LC, West); 0–0.580 ^{a,b} (GWR, N ^{ms} = 877)
Liu et al. (2009) [23]	U.S.	2003–2005	GEOS	GAM	0.790 ^{a,b} (Adjusted, N ^{ms} = 32), 0.480 ^{a,b} (Unadjusted, N ^{ms} = 32); 0.780 ^{*,a,b} (Adjusted, N ^{ms} = 32), 0.460 ^{*,a,b} (Unadjusted, N ^{ms} = 32)
Paciorek et al. (2009) [53]	U.S.	2004	MODIS, MISR, GEOS	GAM	0.573 ^{a,b} (MODIS, Yearly), 0.572 ^{a,b} (GEOS, Yearly); 0.825 ^{a,b} (MODIS, Monthly), 0.825 ^{a,b} (GEOS, Monthly)
Schaap et al. (2009) [54]	Netherlands	2006–2007	MODIS	MLR	0.518 ^{a,b}
Zhang et al. (2009) [21]	U.S.	2005–2006	MODIS	MLR	0.600 ^{a,b} (Southeast U.S.), 0.200 ^{a,b} (Southwest U.S.), (N ^{ms} = 521 for U.S.)
Di Nicolantonio et al. (2010) [55]	Italy	2007	MODIS	CTM	0.680 ^{a,b} (Terra MODIS, N ^{ms} = 23), 0.590 ^{a,b} (Aqua MODIS, N ^{ms} = 23), 0.700 ^{a,b} (Terra and Aqua MODIS, N ^{ms} = 23)
Leon et al. (2010) [25]	Europe, Africa	2006–2008	POLDER	MLR	0.250 ^{a,b} (N ^{ms} = 28)
Tian et al. (2010) [56]	Canada	2004	MODIS	Semi-empirical model	0.650 ^{a,b} (Hourly, N ^{ms} = 30)
van Donkelaar et al. (2010) [57]	Global	2001–2006	MODIS, MISR	CTM	0.593 ^{a,b} (North America, N ^{ms} = 1057), 0.689 ^{a,b} (Elsewhere, N ^{ms} = 244)
Wang et al. (2010) [58]	China	2007–2008	MODIS	LC	0.470 ^a (N ^{ss} = 1, N ^{ms} = 20)
Hu et al. (2011) [59]	U.S.	2003–2004	MODIS	GWR, LC	0–1 ^{a,b} (GWR, N ^{ms} = 877), 0.449 ^{a,b} (LC, N ^{ms} = 877)
Hystad et al. (2011) [60]	Canada	2006	MODIS, MISR	LUR	0.460 ^{*,a,b} (N ^{ms} = 177)
Kloog et al. (2011) [33]	U.S.	2000–2008	MODIS	MEM	0.830 ^{*,a,b} (with available AOD, N ^{ms} = 78), 0.810 ^{*,a,b} (without available AOD, N ^{ms} = 78)
Lee et al. (2011) [19]	U.S.	2003	MODIS	MEM	0.970 ^{a,b} (N ^{ms} = 26), 0.920 ^{*,a,b} (N ^{ms} = 26)
Wu et al. (2011) [61]	China	2007–2008	MODIS	ANN	0.030 ^{a,b} (Hourly in summer, N ^{ms} = 10), 0.580 ^{a,b} (Hourly in winter, N ^{ms} = 10)
Chudnovsky et al. (2012) [35]	U.S.	2003	GEOS	MEM	0.970 ^{a,b} (N ^{ms} = 26), 0.920 ^{*,a,b} (N ^{ms} = 26)
Hystad et al. (2012) [62]	Canada	1975–1994	MODIS, MISR	CTM	0.670 ^{a,b} (N ^{ms} = 25)
Kloog et al. (2012) [34]	U.S.	2000–2008	MODIS	MEM	0.850 ^{*,a,b} (N ^{ss} = 8, N ^{ms} = 161)
Lee et al. (2012) [63]	U.S.	2001–2006	MODIS, MISR	CTM	0.200–0.820 ^{a,b}

Table 1. Cont.

Author (Published Year)	Study Area	Study Period	Source of AOD	Retrieved Model	R ² of Model (CV-R ²)
Lee et al. (2012) [64]	U.S.	2000–2008	MODIS	MEM	0.930 ^{a,b} (MEM for available AOD, N ^{ms} = 69), 0.880 ^{*,a,b} (MEM for available AOD, N ^{ms} = 69)
Liu et al. (2012) [65]	China	2008	MODIS	GAM	0.563 ^a (Adjusted, N ^{ss} = 1, N ^{ms} = 3); 0.757 ^a (Unadjusted, N ^{ss} = 1, N ^{ms} = 3); 0.372 ^{*,a} (Adjusted, N ^{ss} = 1, N ^{ms} = 3), 0.608 ^{*,a} (Unadjusted, N ^{ss} = 1, N ^{ms} = 3)
Mao et al. (2012) [66]	U.S.	2005	MODIS	LUR	0.648 ^{a,b} (Unadjusted, N ^{ms} = 34), 0.626 ^{a,b} (Adjusted, N ^{ms} = 34), 0.58 ^{*,a,b} (N ^{ms} = 34)
van Donkelaar et al. (2012) [67]	U.S.	2004–2009	MODIS, MISR	CTM	0.689 ^b (for day of June 27, 2005. N ^{ms} = 1482)
Wu et al. (2012) [68]	China	2007–2008	MODIS	ANN	0.430 ^{a,b} (N ^{ms} = 7)
Beckerman et al. (2013) [69]	U.S.	2001–2006	-	LUR	0.650 ^{*,a,b} (Monthly, N ^{ms} = 4119)
Beckerman et al. (2013) [70]	U.S.	1991–2008	GEOS	LUR	0.630 ^{*,a,b} (LUR, N ^{ms} = 1464), 0.790 ^{*,a,b} (LUR and BMEM, N ^{ms} = 1464)
Chudnovsky et al. (2013) [71]	U.S.	2003	MODIS	LC	0.470 ^a (New England), 0.620 ^a (Boston), N ^{ms} = 26 for U.S.
Chudnovsky et al. (2013) [72]	U.S.	2002–2008	MODIS	MEM	0.500 ^{*,a,b} (New England), 0.860 ^{*,a,b} (Boston), N ^{ms} = 26 for U.S.
Cordero et al. (2013) [73]	U.S.	2005–2006	MODIS, GEOS	MLR	0.860 ^a (Urban areas in summer, N ^{ms} = 39)
Hu et al. (2013) [74]	U.S.	2003	MODIS	GWR	0.600 ^{a,b} (NARR, N ^{ms} = 119), 0.610 ^{a,b} (NLDAS, N ^{ms} = 119), 0.672 ^{*,a,b} (NARR, N ^{ms} = 119), 0.706 ^{*,a,b} (NLDAS, N ^{ms} = 119)
Kumar et al. (2013) [75]	U.S.	2000–2009	MODIS	MLR	0–1 ^{a,b} (N ^{ms} = 5)
Saunders et al. (2013) [76]	U.S.	2003–2007	MODIS	MLR	0.760 ^{a,b} (Winter)
Strawa et al. (2013) [77]	U.S.	2004–2008	MODIS	GAM	0.770 ^{a,b}
Tao et al. (2013) [17]	China	2007–2008	MODIS	MLR	0.610 ^{a,b} (Beijing and its surrounding regions, N ^{ms} = 17)
Chang et al. (2014) [78]	U.S.	2003–2005	MODIS	LUR	0.780 ^{*,a,b} (N ^{ms} = 85)
Chiu et al. (2014) [79]	U.S.	2002–2009	MODIS	MEM	0.830 ^{*,a,b} (with available AOD, N ^{ms} = 78); 0.810 ^{*,a,b} (without available AOD, N ^{ms} = 78)
Hu et al. (2014) [80]	U.S.	2003	MODIS	TSM	0.830 ^{a,b} , 0.670 ^{*,a,b}
Hu et al. (2014) [81]	U.S.	2001–2010	MODIS, MISR	TSM	0.710–0.850 ^{a,b} (for year 2001–2010), 0.62–0.78 ^{a,b} (for year 2001–2010)
Kloog et al. (2014) [82]	U.S.	2003–2011	MODIS	MEM	0.880 ^{*,a,b} (N ^{ms} = 161)
Kloog et al. (2014) [83]	U.S.	2000–2006	MODIS	MEM	0.810 ^{*,a,b} (N ^{ms} = 161)
Kim et al. (2014) [84]	Korea	2001–2010	MODIS	CTM	0.440 ^{*,a,b} (for PM _{2.5} sulphate), 0.370 ^{*,a,b} (for PM _{2.5} dust), 0.230 ^{*,a,b} (for PM _{2.5} smoke)
Lai et al. (2014) [85]	Global	2012	MODIS	MLR	0.850 ^{a,b} (The best, N ^{ms} = 31)

Table 1. Cont.

Author (Published Year)	Study Area	Study Period	Source of AOD	Retrieved Model	R ² of Model (CV-R ²)
Lary et al. (2014) [28]	Global	1997–2014	Sea WIFS, MODIS	Machine-learning regression	0.920 ^{a,b} (N = 8329)
Lee et al. (2014) [86]	U.S.	2000–2008	MODIS	MEM	0.890 ^{a,b} (for retrieval days, N ^{ms} = 69), 0.860 ^{*,a,b} (for retrieval days, N ^{ms} = 69), 0.790 ^{*,a,b} (for non-retrieval days, N ^{ms} = 69)
Ma et al. (2014) [87]	China	2012–2013	MODIS, MISR	GWR	0.710 ^{a,b} (N ^{ss} = 113, N ^{ms} = 835), 0.640 ^{*,a,b} (N ^{ss} = 113, N ^{ms} = 835)
Rush et al. (2014) [88]	U.S.	2001	MODIS	Kriging	0.815 ^b (Northeast summer); 0.800 ^b (Industrial Midwest summer)
Song et al. (2014) [89]	China	2012–2013	MODIS	GWR	0.738 ^{a,b} (PRD, N ^{ms} = 37)
Toth et al. (2014) [30]	U.S.	2008–2009	MODIS, MISR, CALIOP	LC	0.130 ^{a,b} (Aqua MODIS, Hourly, N ^{ms} = 102), 0.090 ^{a,b} (Terra MODIS, Hourly, N ^{ms} = 102), 0.090 ^{a,b} (MISR, Hourly, N ^{ms} = 102); 0.040 ^{a,b} (Aqua MODIS, Daily, N ^{ms} = 991), 0.063 ^{a,b} (Terra MODIS, Daily, N ^{ms} = 991), 0.063 ^{a,b} (MISR, Daily, N ^{ms} = 991)
Chan et al. (2015) [90]	U.S.	2003–2009	MODIS	Kriging	0.880 ^{*,a,b}
Coker et al. (2015) [91]	U.S.	1995–2006	-	LUR	0.650 ^{*,a,b}
Geng et al. (2015) [92]	China	2006–2012	MODIS, MISR	CTM	0.548 ^{a,b} (N ^{ms} = 46)
Han et al. (2015) [93]	China	2011	MODIS	MLR	0.624 ^a (All dust data but filter out aloft-dust-layer, N ^{ss} = 1); 0.548 ^a (All non-dust data, N ^{ss} = 1)
Just et al. (2015) [94]	Mexico	2004–2014	MODIS	MEM	0.724 ^{*,a} (N ^{ss} = 1, N ^{ms} = 12)
Kloog et al. (2015) [95]	Israel	2003–2013	MODIS	MEM	0.720 ^{*,a,b} (N ^{ms} = 45)
Leon Hsu et al. (2015) [96]	U.S.	2002–2009	MISR	MEM	0.830 ^{*,a,b} (with available AOD, N ^{ms} = 78), 0.810 ^{*,a,b} (without available AOD, N ^{ms} = 78)
Lee et al. (2015) [12]	U.S.	2007–2011	MODIS	MEM	0.770 ^{*,a,b} , 0.810 ^{*,a,b} , 0.700 ^{*,a,b} for region 1, 2, 3 (N ^{ms} = 277)
Lee et al. (2015) [7]	U.S.	2003–2011	MODIS	MEM	0.770 ^{*,a,b} , 0.810 ^{*,a,b} , 0.700 ^{*,a,b} for region 1, 2, 3 (N ^{ms} = 257)
Li et al. (2015) [29]	U.S.	2005–2010	MODIS, MISR, SeaWiFS, OMI	CMCA, MCA	CMCA: 0.600 ^{a,b} (MODIS/MISRR/SeaWiFS/OMI, N ^{ms} = 98), 0.792 ^{a,b} (for year between 2005 and 2010, N ^{ms} = 198); MCA: 0.828 ^{a,b} (for year between 2005 and 2010, N ^{ms} = 98)
Lin et al. (2015) [97]	China	2013	MODIS	Semi-empirical model	0.810 ^{a,b} (N ^{ms} = 565, Yearly), 0.578 ^{a,b} (N ^{ms} = 565, Monthly)
McHenry et al. (2015) [98]	U.S.	2002	MODIS	CMAQ	0.468 ^{a,b} (yearly)
Nguyen et al. (2015) [99]	Vietnam	2011–2012	MODIS	SVR, MLR	0.352 ^{a,b} (SVR), 0.358 ^{a,b} (MLR)
Song et al. (2015) [100]	China	2013	MODIS	GAM	0.691 ^a (N ^{ss} = 1, N ^{ms} = 13)
van Donkelaar et al. (2015) [101]	U.S.	2004–2008	MODIS	CTM	0.620 ^{a,b} (Unadjusted, N ^{ms} = 1253), 0.820 ^{a,b} (Adjusted, N ^{ms} = 1253), 0.780 ^{*,a,b} (N ^{ms} = 1253)

Table 1. Cont.

Author (Published Year)	Study Area	Study Period	Source of AOD	Retrieved Model	R ² of Model (CV-R ²)
van Donkelaar et al. (2015) [27]	Global	1998–2012	MODIS, MISR SeaWiFS	CTM	0.656 ^{a,b} (North America and Europe, N ^{ms} = 210)
Wong et al. (2015) [102]	China	2000–2011	-	SEC	0.360
Xie et al. (2015) [103]	China	2013–2014	MODIS	MEM	0.810–0.830 ^a (various between districts, N ^{ss} = 1, N ^{ms} = 35), 0.750–0.790 ^{*,a} (various between districts, N ^{ss} = 1, N ^{ms} = 35)
Xu et al. (2015) [104]	China	2013	GOCI	CTM	0.656 ^{a,b} (Yearly, N ^{ms} = 494)
You et al. (2015) [105]	China	2013	MODIS, MISR	Nonlinear regression model	0.670 ^a (MODIS, N ^{ss} = 1, N ^{ms} = 13), 0.720 ^a (MISR, N ^{ss} = 1, N ^{ms} = 13)
Zhang et al. (2015) [106]	China	2013	MODIS	MLR	0.462 ^a (Hourly, N ^{ss} = 1, N ^{ms} = 15)
Bai et al. (2016) [107]	China	2015	MODIS	GTWR, OLS, GWR, TWR	0.960 ^{a,b} (GTWR, N ^{ms} = 37), 0.870 ^{*,a,b} (GTWR, N ^{ms} = 37); 0.350 ^{a,b} (OLS, N ^{ms} = 37), 0.410 ^{a,b} (OLS, N ^{ms} = 37); 0.590 ^{a,b} (GWR, N ^{ms} = 37), 0.600 ^{a,b} (GWR, N ^{ms} = 37); 0.630 ^{a,b} (TWR, N ^{ms} = 37), 0.680 ^{a,b} (TWR, N ^{ms} = 37)
Beloconi et al. (2016) [108]	UK	2002–2012	MODIS	Kriging, MEM	0.040 ^{*,a} (Kriging, N ^{ss} = 1), 0.846 ^{*,a} (MEM, N ^{ss} = 1)
Crouse et al. (2016) [109]	Canada	2001–2010	MODIS, MISR, SeaWiFS	CTM	0.578 ^{a,b}
Di et al. (2016) [110]	U.S.	2000–2012	MODIS	ANN	0.840 ^{*,a,b} (N ^{ms} = 1928)
Di et al. (2016) [111]	U.S.	2001–2010	-	ANN	0.850 ^{**a,b} (N ^{ms} = 154)
Girguis et al. (2016) [112]	U.S.	2001–2008	MODIS	MEM	0.780–0.880 ^{*,a,b} (for year 2001–2008, N ^{ms} = 35)
He et al. (2016) [113]	China	2014–2015	MODIS	LC	0.723 ^{a,b} (N ^{ss} = 6, N ^{ms} = 82)
Kloog et al. (2016) [114]	U.S.	2000–2008	MODIS, MISR	MEM	0.820 ^{*,a,b}
Karimian et al. (2016) [115]	China	2013	MODIS	Improved LC	0.500 ^a (Terra MODIS, N ^{ss} = 1, N ^{ms} = 8), 0.566 ^a (Aqua MODIS, N ^{ss} = 1, N ^{ms} = 8)
Lee et al. (2016) [116]	U.S.	2006–2012	MODIS	MEM	0.666 ^{*,a,b} (N ^{ms} = 87)
Lin et al. (2016) [117]	China	2000–2014	MODIS	LC	0.672 ^{a,b} (Monthly, 2000–2014, N ^{ms} = 3094), 0.608 ^{a,b} (Yearly, 2013, N ^{ms} = 76), 0.548 (Yearly, 2014, N ^{ms} = 86)
Lv et al. (2016) [118]	China	2014	MODIS	Bayesian model	0.780 ^{*,a,b} (N ^{ss} = 53, N ^{ms} = 298)
Ma et al. (2016) [87]	China	2013	MODIS	Improved MEM	0.725 ^{*,a,b} (Nested MEM, N ^{ss} = 5, N ^{ms} = 115), 0.724 ^{*,a,b} (Non-nested MEM, N ^{ss} = 5, N ^{ms} = 115); 0.486 ^{**a,b} (Nested MEM, N ^{ss} = 5, N ^{ms} = 115), 0.230 ^{**a,b} (Non-nested MEM, N ^{ss} = 5, N ^{ms} = 115)
Ma et al. (2016) [119]	China	2004–2013	MODIS	TSM	0.790 ^{*,a,b} (N ^{ss} = 205, N ^{ms} = 1185)
Shi et al. (2016) [120]	U.S.	2003–2008	MODIS	MEM	0.870 ^{*,a,b}
Strickland et al. (2016) [121]	U.S.	2002–2010	MODIS	TSM	0.710–0.85 ^{a,b} (Yearly)

Table 1. Cont.

Author (Published Year)	Study Area	Study Period	Source of AOD	Retrieved Model	R ² of Model (CV-R ²)
Stieb et al. (2016) [122]	Canada	1999–2008	MODIS	LUR	0.590 ^{*,a,b} (N ^{ms} = 241)
van Donkelaar et al. (2016) [123]	Global	1998–2014	MODIS, MISR, SeaWiFS	CTM and GWR	0.810 ^{*,a,b}
Wang et al. (2016) [124]	Canada	2009	MODIS	CTM	0.860 ^a (Daily, N ^{ss} = 1, N ^{ms} = 10), 0.930 ^a (Monthly, N ^{ss} = 1, N ^{ms} = 10)
You et al. (2016) [125]	China	2014	MODIS	GWR	0.810 ^{a,b} (N ^{ms} = 943), 0.790 ^{*,a,b} (N ^{ms} = 943)
You et al. (2016) [126]	China	2014	MODIS, MISR	GWR	0.760 ^{*,a,b} (MODIS, N ^{ms} = 943), 0.810 ^{*,a,b} (MISR, N ^{ms} = 943)
Zheng et al. (2016) [127]	China	2013	MODIS	MEM	0.770 ^{*,a,b} (BTH, N ^{ss} = 3, N ^{ms} = 66), 0.800 ^{*,a,b} (YRD, N ^{ss} = 15, N ^{ms} = 56), 0.800 ^{*,a,b} (PRD, N ^{ss} = 11, N ^{ms} = 55)
Zou et al. (2016) [128]	China	2013	MODIS	GWR, OLS	0.750 ^{a,b} (GWR, N ^{ss} = 3, N ^{ms} = 52), 0.530 ^{a,b} (OLS, N ^{ss} = 3, N ^{ms} = 52)

* Sample-based CV-R²: Sample-based Cross Validated-coefficient of determination; ** DOY-based CV-R²: Day-of Year-based Cross Validated-coefficient of determination; ^{a,b} denotes Temporal and Spatial of R², respectively; R² denotes daily PM_{2.5} expect for note with monthly and yearly; N^{ms} denotes number of PM_{2.5} monitoring site; N^{ss} denotes number of study site at city level. The list of abbreviations: (1) Satellite Sensors: MODIS, Moderate Resolution Imaging Spectrometer; MISR, Multi-Angle Imaging Spectrometer; GEOS, Geostationary Operational Environment Satellite; SeaWiFS, Sea-viewing Wide Field-of-view Sensor; POLDER, Polarization of Earth's Reflectance and Directionality; CALIOP, Cloud-Aerosol Lidar with Orthogonal Polarization; GOCI, Geostationary Ocean Color Imager; OMI, Ozone Monitoring Instrument; (2) Derived models: LC, Linear Correlations; MLR, Multiple Linear Regression; LUR, Land Use Regression; GAM, Generalized Additive Model; MEM, Mixed-Effect Model; CTM, Chemical Transport Model; GLM, General Linear regression Model; ANN, Artificial Neural Networks; TSM, Two-Stage Model; SVR, Support Vector Regression; GTWR, Geographically and Temporally Weighted Regression; TWR, Temporally Weighted Regression; TVM, Two-Variate Method; MVM, Multivariate Method; OLS, Ordinary Least Squares model; SEC, Surface Extinction Coefficient; Nested MEM, Nested Mixed Effects Model; Non-nested MEM, Non-nested Mixed Effects Model; DSA, Deletion/substitution/addition; BMEM, Bayesian Maximum Entropy method; MCA, Maximum Covariance Analysis; CMCA, Combined Maximum Covariance Analysis (3) R² of model, Coefficient of determination of model: NARR, North American Regional Reanalysis; NLDAS, North American Land Data Assimilation System; BTH, Beijing-Tianjin-Hebei region; YRD, Yangtze River Delta region; PRD, Pearl River Delta region.

Of these 116 studies, 25 used Multiple Linear Regression (MLR), 23 used the Mixed-Effect Model (MEM), 16 used the Chemical Transport Model (CTM), and 10 used Geographically Weighted Regression (GWR), while Linear Correlations (LC), the Generalized Additive Model (GAM), Land Use Regression (LUR) and others models were found in 12 studies, six studies, seven studies and 27 studies, respectively (Figures 2 and 3).

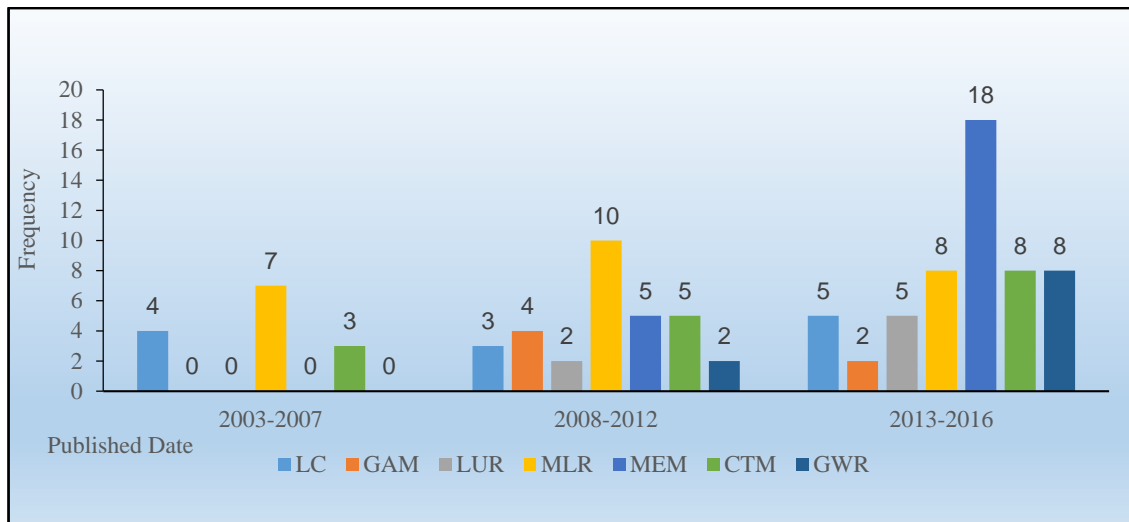


Figure 2. The frequency distribution of seven models.

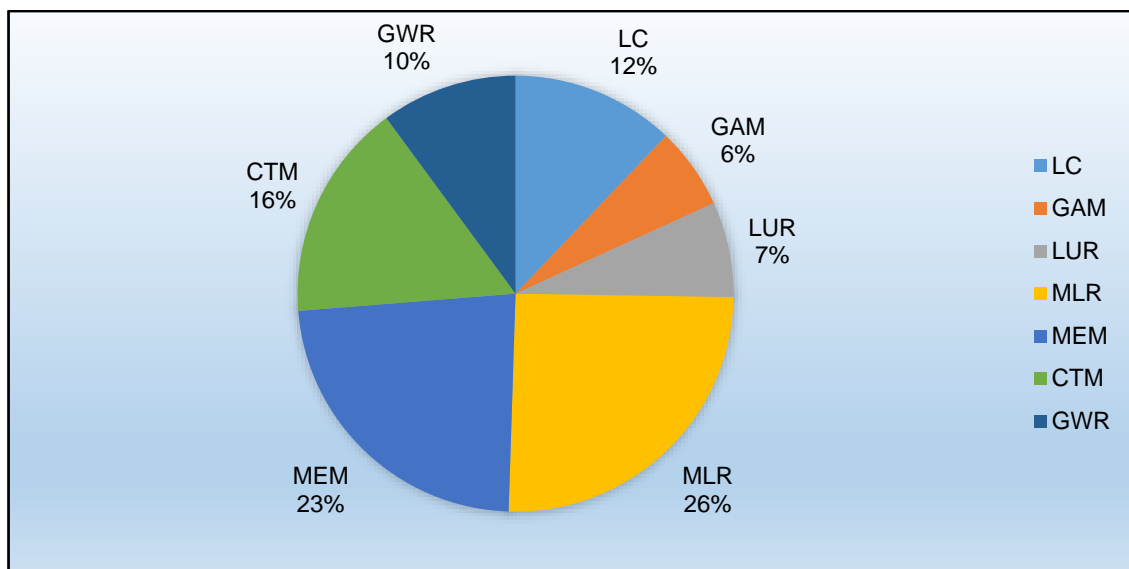


Figure 3. Constituent ratio of seven models.

4. Discussion

Satellite remote sensing technology plays an essential role in the field of meteorology because of its highly accurate prediction of meteorological disasters. Recently, this technology has also been used in the prediction of daily air pollution (PM_{2.5}) levels. Although PM_{2.5} data can be obtained from AOD measured by ground-based remote sensing equipment [129], it is more meaningful to predict PM_{2.5} levels from satellite observations. From our study, we concluded that MLR, MEM, CTM, and GWR were the models most commonly used to predict PM_{2.5} levels.

4.1. Multiple Linear Regression

4.1.1. Theory Background and Application

MLR has been used to predict $PM_{2.5}$ from satellite AOD since 2005. In this model, $PM_{2.5}$ measured at ground level $PM_{2.5}$ was set as the dependent variable, and AOD was set as the independent variable. Several factors were also included in the model as covariates, including humidity, temperature, wind speed, wind direction, aerosol type, and height of the boundary layer. MLR was often used in earlier studies to predict $PM_{2.5}$ levels. For instance, Liu et al. [38] used this model to analyze three area types (city, and suburb and countryside) in the eastern United States in 2001. They reported that coefficients were quite low to some extent and also varied greatly between different regions; R^2 values were 0.420, 0.490, 0.590 and 0.430 in city, suburban, countryside and whole area, respectively. The low R^2 value showed above indicated that the inclusion of covariates (such as relative humidity, height of the boundary layer, season variable, etc.) in MLR models requires further discussion [33]. In contrast, R^2 value reached up to 0.960 in Gupta's study when certain conditions (weather condition, boundary layer heights and others conditions) were met [41].

More recently, in order to improve model performance, some studies have explored covariate factors in the MLR model under different conditions [17,20,21,24–26,39–41,46,47,49,50,54,75]. A few covariate factors, such as relative humidity and height of the boundary layer, were regarded as significant enough to affect and even invert the relationships between AOD and $PM_{2.5}$. In 2013, Cordero et al. [73] predicted $PM_{2.5}$ levels by applying both the satellite-based MLR method and the Community Multi-Scale Air Quality (CMAQ) model. Results showed that the satellite-based MLR method performed better than the CMAQ model during summer: R^2 values ≥ 0.423 (MODIS), R^2 values ≥ 0.137 (CMAQ). However, the R^2 value increased to 0.740 when the two models were combined [73]. In 2015, Han et al. carried out affecting factors analyses between AOD and $PM_{2.5}$ in Nanjing [93]. The authors found that aerosol type and height of the boundary layer were significant factors in the prediction of $PM_{2.5}$ levels. They also stated that R^2 value was 0.624 with only aerosol type adjusted, and R^2 value was 0.548 when both aforementioned significant factors were adjusted [93].

4.1.2. Advantages and Disadvantages

In summary, the determination coefficients of MLR were relatively higher than those of the linear correlation model, and a confounding bias could be avoided by including relevant covariates into the model. However, there are several limitations. Some important covariates, such as seasonal variation of the aerosol, regional variation, and land use information, were missing from the models [93]. Additionally, the accuracy and resolution of the satellite-derived AOD and meteorological data was low [38], which can lead to an information bias.

4.2. Mixed-Effect Model

4.2.1. Theory Background and Application

In early research, missing AOD data was an essential factor in the estimation of $PM_{2.5}$ from AOD, and the method used to compensate for missing AOD data is a very important factor in the precision and accuracy of the derivation. Kloog et al. [33], from Harvard School of Public Health, first proposed that satellite-derived AOD could be included in the three-stage MEM and they applied this approach in New England in 2011. Based on the AOD day-specific correction mixed-effect model of Lee et al. [19], they took meteorological variables and classic land use variables into the MEM [34]. The MEM also used the inverse distance weight method (IDW), cluster analysis, GAM and generalized additive mixed model (GAMM) to deal with missing AOD values so that daily ground $PM_{2.5}$ levels could be predicted in a wide range [34]. If missing AOD presented non-random distribution, AOD data needed to be corrected by meteorological factors using the inverse probability weight method (IPW) [82].

MEM has been applied in many regions. In New England, Kloog et al. [33] constructed their own MEM, based on MEM of Lee et al., in 2011 (CV R^2 value = 0.830, for days with available AOD data; 0.810, for days without AOD data). The distinctive feature of the model of Kloog et al. is its inclusion of meteorological variables (such as temperature, wind speed and visibility) and land use variables (such as elevation, percentage of open spaces, area emissions, point emissions and distance to major roads) into the model, which is appropriate for studying acute and chronic health effects. Since then, many researchers, including Kloog, Madrigano, Chiu and others, have used MEM to study acute and chronic health effects [79,96,130–133], and it has performed well. In 2012, by using GEOS AOD data and adding a surface reflection variable into MEM, Chudnovsky et al. [35] showed a high predictive value of CV- R^2 = 0.920. This study also proved that high resolution GEOS AOD may be a better predictor of urban $PM_{2.5}$ than rough resolution MODIS AOD [35]. Lee et al. [64] found that the R^2 value of MEM could reach 0.830 if missing AOD value were filled using a combination of cluster analysis and generalized additive models. In the mid-Atlantic region, Kloog et al. [34] improved the MEM by adopting IPW for non-random missing AOD data, and obtained a value of 0.850 for the cross-validation of R^2 . Kloog et al. [34] also established $PM_{2.5}$ predictive models in different regions by adding traffic density, population density and distance to the point emission variables.

In 2013, in order to take advantage of high resolution AOD products. Chudnovsky et al. [56] developed a MODIS based Multi-Angle Implementation of Atmospheric Correction algorithm (MAIAC) and used this new algorithm to improve the inversion resolution of MODIS AOD products (from 10×10 km to 1×1 km). In their results, R^2 value reached up to 0.500 in New England and 0.860 in Boston area [72]. The MAIAC algorithm has since been widely applied in MEM studies [7,82,83,94,120,134]. Kloog et al. [83] obtained a CV- R^2 value of 0.810 in mid-western United States in 2000–2006. In a later study based on an early MEM [33,34], Kloog et al. performed a GAM to address missing AOD values, obtaining an R^2 value of 0.880 in the northeastern United States (New England, New York and New Jersey) [82]. In New England, Alexeeff et al. [135] further employed the MEM model with [34,131] Kriging and land use regression to describe an epidemiological relationship between AOD and predicted $PM_{2.5}$ in 2003. The following year, Shi et al. [120] used MEM to predict $PM_{2.5}$ using MODIS AOD data collected between 2003 and 2008, and they obtained consistent results (R^2 value = 0.890) for days with available AOD data and without available AOD data. This method was also successfully applied in studies on the relationship between low $PM_{2.5}$ exposure and mortality.

In recognition of regional geographical differences, Lee et al. [7] predicted $PM_{2.5}$ concentrations using IPW in seven southeastern states of the United States in 2016, and they obtained three coefficients of determination (0.770, 0.810, and 0.700) from three different geographical area types. They suggested that their $PM_{2.5}$ estimation methods could be applied from urban areas to rural areas. Just et al. [94] analyzed the geographical distribution of $PM_{2.5}$ in Mexico in 2004–2014. They obtained an R^2 value of 0.724 using MEM and showed that precipitation and height of the boundary layer are both important factors influencing the relationship between AOD and $PM_{2.5}$ [94]. Furthermore, with AOD derived from Medium Resolution Imaging Spectrometer (MERIS) and Advanced Along-Track Scanning Radiometer (AATSR) synergistic observations. Beloconi et al. [108] applied MEM to the evaluation of the day-specific and site-specific random effects in London. Their results showed a CV- R^2 value of 0.846 between 2002 and 2012. Ma et al. [136] provided an improved MEM to address data missing from satellite observation as well as ground-level measurements.

4.2.2. Advantages and Disadvantages

To sum up, MEM had the following advantages: (1) It had a relatively high predicting coefficient of determination. The R^2 value could generally reach up to 0.800 or higher. R^2 values of time and spatial consistency were also high; they could reach up to 0.700 or higher among different regions. Besides, R^2 value could be greatly enhanced through the use of MAIAC algorithms [7,72,82]; (2) MEM could be widely applied to the prediction of $PM_{2.5}$ at a regional level by using different land use

and meteorological variables for model calibration; (3) MEM can be used to predict daily $PM_{2.5}$ concentrations, and has been applied in studies on the acute and chronic health effects of $PM_{2.5}$ exposure in New England, the Mid-Atlantic and other regions of the United States. These studies can be extended to other regions in the future [15]. The model may also be used to explore the difference between satellite-derived AOD-based $PM_{2.5}$ data and ground based $PM_{2.5}$ data in health effect studies.

MEM has the following disadvantages: (1) Due to the lack of ground-level $PM_{2.5}$ monitoring data in certain areas, the $PM_{2.5}$ monitoring data could not meet the requirements of Kriging in MEM, which affected the accuracy of the results [72]; (2) The determination of correlation between AOD and $PM_{2.5}$ may decrease when only total AOD is applied. It is not clear which of the aerosols influencing AOD (such as sulfate, nitrate, ammonium, carbonaceous, mineral dust, and sea salt) plays a major role in the total AOD, or how much other air pollutants affect this correlation [33,94,137]; (3) Land use and traffic pollution information is hard to collect.

4.3. Chemistry Transport Model

4.3.1. Theory Background and Application

Based on the characteristics of vertical distribution and transmission of AOD, Liu et al. [18] proposed the Global atmospheric chemistry model (GEOS-CHEM), which is a prediction model of $PM_{2.5}$ based on satellite AOD. Following Liu and coworkers' study [138], van Donkelaar et al. [43] developed the CTM which calibrates the height of the boundary layer and the humidity of air. Considering the composition and distribution of AOD and utilizing emissions listing data as well as daily emission patterns published in European and other countries, van Donkelaar et al. built a precise CTM formula in 2006. In 2010, they simplified the CTM by redefining the association between AOD and $PM_{2.5}$ as a conversion factor. CTM can now be used on a global as well as a local scales [6,57], and has attracted extensive interest [139,140].

This model was employed in different regions between 2010 and 2012. Di Nicolantonio and Cacciari [55] applied the method in North Italy and obtained different results for satellite-based $PM_{2.5}$ predicting results (R^2 values of 0.680 (Terra MODIS), 0.590 (Aqua MODIS), 0.700 (Terra and Aqua MODIS, respectively). Hystad et al. [62] obtained an R^2 value of 0.410 for the first time to add land use variables in Canada using CTM [57]. Additionally, in a comparison between IDW-adjusted CTM and MLR, IDW-adjusted CTM (R^2 value = 0.510 per year) performed better than MLR (R^2 value = 0.330 per year) [62,67]. Lee et al. [63] made a comparison between the Kriging method and CTM in the United States. Although both methods gave consistent results, CTM had better applicability and higher accuracy, especially in areas with few ground level monitoring sites. Further studies by van Donkelaar et al. have shown that meteorological factors can calibrate and reduce the system error and spatial smoothing of the IDW method can reduce the random error, eventually extending the spatiotemporal prediction scale [67]. Crouse [141] not only obtained a high R^2 value (0.792) in 11 Canadian cities in 1987–2001, but also successfully applied their results to the study of long-term health effects of $PM_{2.5}$ exposure. Following van Donkelaar's study [57], others studies conducted by Villeneuve, Chen, To and Brauer [142–146] focused on acute and chronic health effects and on the global burden of disease.

In addition, the estimates of $PM_{2.5}$ from MODIS AOD in the above studies were somewhat varied. In 2013, van Donkelaar et al. [147] added land use type data, which were used to quantify the weight of AOD data, and proposed Optimal Estimation (OE) in order to improve the predictive ability of AOD. More recently, Wang et al. [124] have provided an improved AOD retrieval algorithm for MODIS at 1 km resolution that can be retrieve AOD at high spatial resolutions at intra-urban scales. These MODIS-retrieved AODs are used to predict ground level $PM_{2.5}$ using aerosol vertical profiles and local scale factors obtained from the CTM simulation. Daily R^2 value = 0.860 and monthly R^2 value = 0.930 were obtained from data collected over the city of Montreal, Canada [124].

At the global level, in a study similar to van Donkelaar's 2010 study, Boys and Martin [148] completed a global ground level prediction of PM_{2.5} in 2014, which integrated global AOD data collected from the MISR and SeaWiFS AOD (1 km × 1 km) satellite sensor between 1998 and 2012. They also included a few effecting factors in the CTM, such as the vertical structure of aerosol extinction, relative humidity, aerosol size and component of aerosol variables. Their results showed that PM_{2.5} levels in East America, the Arabian Peninsula, Eastern and southern Asia were relatively consistent [148]. In a different study, van Donkelaar et al. [101] combined GWR with CTM, and obtained a higher value of CV-R² (0.780) with high resolution in North America. In the same year, van Donkelaar et al. [27] improved the CTM approach to the prediction of PM_{2.5} concentrations at a global level. Their research integrated AOD data from three satellites in order to avoid negative effects from the source variations of AOD. The study obtained high R² values (0.656) for North America in 2001–2010, indicating that PM_{2.5} prediction could be feasible at the global level.

4.3.2. Advantages and Disadvantages

Based on above studies, the advantages of CTM are: (1) it can predict PM_{2.5} concentrations at ground level without PM_{2.5} data from ground monitors [127]; and (2) it takes the component of AOD and the effects of other pollutants into account, and has been widely used in Canada, North America and South America, for predicting on a global scale [27,28,149,150]. CTM is currently central to health effect analysis related to PM_{2.5} components [109]. The disadvantages of CTM are: (1) the prediction effect was relatively low and variant among different regions. Considering the poor performance of CTM, lower R² values can lead to a high exposure bias in health effect studies; (2) it will consume time, energy and financial resources to collect the necessary chemical and physical information on PM_{2.5} [57]; (3) due to the lack of pollutants emissions type and emissions listing data in developed countries, it is hard to meet the conditions of application of CTM in China, India and other developing countries [27]; and (4) other pollutants (SO₂, O₃, etc.) have different inversion resolutions compared with PM_{2.5} [143].

4.4. Geographical Weighted Regression

4.4.1. Theory Background and Application

Based on the assumption that “regression coefficient is a function of the observation point's spatial position in linear regression” with spatial weight assigned according to the distance between observation points, Geographical Weighted Regression (GWR) was first proposed [151,152]. This spatial regression technique reflects spatial variability and non-smooth character, and could provide a regional-level regression model [151–153]. In 2009, Hu et al. [32] introduced AOD into GWR and carried out a prediction of PM_{2.5} levels in the United States. After that, Ma [87] further optimized GWR in 2014 by taking AOD, land use variables as the independent variables, and PM_{2.5} concentrations as the dependent variable. Meanwhile, based on the differences between regions in PM_{2.5} ground monitoring, spatial weight assignment was developed and applied to each region with the quantity of AOD data. If a large proportion of AOD data was missing, we could select certain buffer areas for each spatial observation point and fill in the vacancy according to the corrected Akaike Information Criterion. Thus, spatial distribution of regression parameter gained, and the GWR model could explain the effects of the spatial autocorrelation within a certain area when spatial aggregation occurred for a certain variable [87,105,107,128].

Hu's initial investigation on GWR found that it had a low R² value compared with MEM and CTM, probably because not all studies took meteorological factors and land use factors into account [32]. Based on regional differences, Hu et al. [59] brought meteorological variables and land use variables into the GWR to predict PM_{2.5} concentrations in North America. Results showed that R² values improved significantly when these variables were considered (R² = 0.672 (North American Regional Reanalysis data), and R² = 0.706 (North American Land Data Assimilation System data)). However,

large spatial variability and instability occurred in these variables. Further studies showed that PM_{2.5} concentrations were higher in urban areas, and lower in rural villages or mountain areas.

In order to compensate the basis without considering the cross-validation, Ma et al. [87] expanded the National GWR model with data from the newly built national monitoring network to predict PM_{2.5} levels in China, reporting a CV-R² value of 0.640. This result indicated that it was feasible to estimate PM_{2.5} levels in China using satellite AOD combined with meteorological and land use data. The model obtained similar results to those obtained by the CTM used by van Donkelaar in 2010, but GWR found higher PM_{2.5} concentrations in rural areas. Similar results for national PM_{2.5} levels were found by You et al. [126] with CV-R² values of 0.760 and 0.810 for MODIS and MISR, respectively, in China. Additionally, using 3-km resolution MODIS AOD in 2014, You et al. [125] confirmed that this GWR approach is useful for estimating large-scale ground-level PM_{2.5} distributions in China.

4.4.2. Advantages and Disadvantages

From the studies above, the advantages of this model are: (1) PM_{2.5} estimation requires only small amounts of data. For example, this model can work with the daily average, monthly average or yearly average of both PM_{2.5} data alone or AOD data alone. Determination coefficients were also less affected. Studies have shown that compared with CTM, GWR had a higher R² value [87]; (2) Similar to MEM, GWR used ground monitored PM_{2.5} values for AOD calibration, and it had a better model performance than MLR. The disadvantages are: (1) since model construction depends on ground monitoring data, model performance may be much less reliable in areas lacking ground monitoring data; and (2) to our knowledge, GWR has only been employed in limited PM_{2.5} prediction studies with the combination of satellite data [74,87,100,107,125,126,128], so the feasibility of applying it widely in other regions needs to be investigated in further research.

4.5. Other Models

In addition to the models mentioned above, other researchers used linear correlations [16,30,31,37,42,58,71,113,115,117], GAM [23,24,53,65,77], LUR [66,69,70,78,91,122], Kriging [88,90,108] or the nonlinear regression model. Those PM_{2.5} estimating models all regard AOD as the primary independent variable. As a result, the predictability of these models was limited. Their R² values were generally lower, and varied between different areas. However, these listed models have been gradually optimized or integrated into other models, as with artificial neural networks (ANN, which incorporate LUR in the CTM) [52,61,68,110,111] and the two stage model (TSM, which combine the GWR with MEM) [80,81,119,121]. In recent years, with the development of the AOD-based mathematical model, many new methods have been developed, such as geographically and temporally weighted regression (GTWR) [107], support vector regression methods (SVR) [99] and machine learning regression (which is a combination of SVR, Gauss neural network processes, Decision trees, and Random forests) [28]. Although these new methods had been proposed, their reliability and veracity need to be investigated in further studies.

4.6. Summary

In terms of the accuracy of PM_{2.5} prediction, though no single model can replace all others, some existing models have their advantages in the following areas. (1) Model predictability: MLR was commonly used in early studies [17,20,21,24–26,39–41,46,47,49,50,54,75], whereas MEM and CTM gradually became the dominant methods and replaced MLR after 2010. However, GWR has developed at a slower pace with a limited number of studies to data, and had moderate performance [32,74,125,126]. Included studies showed that R² value of MEM was higher than those of the other three models in the same area [17,87,104,136]. Moreover, MAIAC algorithms, which led to a highly accurate of AOD, were mostly used in MEM, significantly improving the R² value of the model [7,35,83,120,135]. On the global scale, CTM has been proven to be efficient for the mechanism of completing the prediction from using partial AOD data by AOD component analysis [57]; (2) Adjusting factors: The number

of these factors has increased due to the development of prediction models. Moreover, factors such as atmospheric boundary layer height and relative humidity have become a permanent part of the adjustment process. In early LC and MLR studies, adjusting factors were limited in number and scope, and were mainly focused on meteorological factors (atmospheric boundary layer height, humidity, temperature, wind speed, etc.) [38,39,41,42]. Later on, GAM took both meteorological factors and land use factors into account, which increased the performances [23,77]. MEM and CTM also incorporated more meteorological factors and land use factors; their R^2 values proved to be satisfactory; (3) Missing AOD: Although predicting of $PM_{2.5}$ with satellite AOD has become the hotspot in remote sensing field, missing values of AOD cannot be ignored, because the predicted reliability of $PM_{2.5}$ could be affected when the percentage of missing AOD values reach 60%. Among the four models, MEM systematically and comprehensively described methods of dealing with missing AOD [137]; results of each method could be found in different studies. CTM, on the other hand, filled in the vacancy by establishing “buffer areas” or avoided the problem of missing AOD by assigning different weights to each area according to the amount of AOD data. For the MLR, missing AOD was not processed.

5. Conclusions

The review showed that MEM performed best. CTM had strengths in the prediction of $PM_{2.5}$ on a global scale. GWR was suitable for $PM_{2.5}$ prediction on a regional scale. MLR was relatively weak in terms of predictability. When land use information was included as an adjustment factor in addition to meteorological factors, the accuracy of predictions greatly improved. Other models, such as ANN, TSM and SVR, need to be further validated. We therefore suggest that the following possibilities be considered in future studies: (1) the use of AOD data with higher resolution for more accurate estimation of $PM_{2.5}$ in relatively small areas; (2) the use of satellite-based predicting models for historical $PM_{2.5}$ prediction and retrospective study in areas lacking historical $PM_{2.5}$ data; and (3) the development prediction models not only for PM but also for other air pollutants (SO_2 , NO_2), to extend the applicability of predicting models.

Acknowledgments: This review was funded by National Natural Science Foundation of China (No. 41571344); the National Key Research and Development Program of China (No. 2016YFC0200900); the Hubei Province Health and Family Planning Scientific Research Project (Grant No. WJ2015Q023); the Fundamental Research Funds for the Central Universities (Grant No. 2042016kf0165); China Postdoctoral Science Foundation (No. 2015M572198); the program of Key Laboratory for National Geographic Census and Monitoring, National Administration of Surveying, Mapping and Geo-information (No. 2014NGCM); Planning Project of Innovation and Entrepreneurship Training of National Undergraduate (No. 201510486102); and Innovation Experiment Program of Medical Students of Wuhan University (No. MS2015037). We express our great thanks to scholars from School of public health, Wuhan University and State Key Laboratory of Information Engineering, Mapping and Remote Sensing, Wuhan University for their helpful suggestion and discussion.

Author Contributions: The study was carried out in collaboration between all authors. Hao Xiang brought idea formation. Yuanyuan Chu, Yisi Liu and Xiangyu Li drafted the manuscript. Zhiyong Liu and Hanson contributed to make the outline, check results of all models and write the discussion part. Xi Chen, Na Li, Meng Ren and Feifei Liu selected articles under the inclusion and exclusion criteria. Yuan'an Lu, Zongfu Mao, Liqiao Tian and Zhongmin Zhu introduced the technologies of deriving $PM_{2.5}$ from Aerosol Optical Depth.

Conflicts of Interest: The authors declare no conflict of interest.

Abbreviations

The following abbreviations are used in this manuscript:

AOD	Aerosol Optical Depth
MODIS	Moderate Resolution Imaging Spectrometer
MISR	Multi-Angle Imaging Spectrometer
GEOS	Geostationary Operational Environment Satellite
SeaWiFS	Sea-viewing Wide Field-of-view Sensor
POLDER	Polarization of Earth's Reflectance and Directionality
CALIOP	Cloud-Aerosol Lidar with Orthogonal Polarization
GOCI	Geostationary Ocean Color Imager
OMI	Ozone Monitoring Instrument (OMI)
AATSR	Advanced Along-Track Scanning Radiometer

MERIS	Medium Resolution Imaging Spectrometer
LC	Linear Correlations
MLR	Multiple Linear Regression
LUR	Land Use Regression
GAM	Generalized Additive Model
MEM	Mixed-Effect Model
CTM	Chemical Transport Model
GLM	General Linear regression Model
GWR	Geographically weighted regression
TWR	Temporally Weighted Regression
GTWR	Geographically and Temporally Weighted Regression
ANN	Artificial Neural Networks
SVR	Support Vector Regression
MCA	Maximum Covariance Analysis
CMCA	Combined Maximum Covariance Analysis
TVM	Two-variate method
MVM	Multivariate method
OLS	Ordinary Least Squares model
TSM	Two-Stage Model
MAIAC	Multi-Angle Implementation of Atmospheric Correction algorithm
DSA	Deletion/Substitution/Addition
BMEM	Bayesian Maximum Entropy method
Nested MEM	Nested Mixed-Effect Model
Non-nested MEM	Non-nested Mixed-Effect Model
SEC	Surface Extinction Coefficient
BTH	Beijing-Tianjin-Hebei region
PRD	Pearl River Delta region
YRD	Yangtze River Delta region
NARR	North American Regional Reanalysis
NLDAS	North American Land Data Assimilation System
Sample-based CV-R ²	Sample-based Cross Validated-coefficient of determination
DOY-based CV-R ²	Day-of-Year-based Cross Validated-coefficient of determination

References

- World Health Organization. 7 Million Premature Death in Annually Linked to Air Pollution. Available online: <http://www.who.int/mediacentre/news/releases/2014/air-pollution/en/> (accessed on 25 March 2014).
- Dockery, D.W. Health effects of particulate air pollution. *Ann. Epidemiol.* **2009**, *19*, 257–263. [[CrossRef](#)] [[PubMed](#)]
- Risom, L.; Moller, P.; Loft, S. Oxidative stress-induced DNA damage by particulate air pollution. *Mutat. Res.* **2005**, *592*, 119–137. [[CrossRef](#)] [[PubMed](#)]
- Hoek, G.; Krishnan, R.M.; Beelen, R.; Peters, A.; Ostro, B.; Brunekreef, B.; Kaufman, J.D. Long-term air pollution exposure and cardio-respiratory mortality: A review. *Environ. Health* **2013**, *12*, 43. [[CrossRef](#)] [[PubMed](#)]
- Brook, R.D.; Rajagopalan, S.; Pope, C.A., 3rd; Brook, J.R.; Bhatnagar, A.; Diez-Roux, A.V.; Holguin, F.; Hong, Y.; Luepker, R.V.; Mittleman, M.A.; et al. Particulate matter air pollution and cardiovascular disease: An update to the scientific statement from the American Heart Association. *Circulation* **2010**, *121*, 2331–2378. [[CrossRef](#)] [[PubMed](#)]
- Lim, S.S.; Vos, T.; Flaxman, A.D.; Danaei, G.; Shibuya, K.; Adair-Rohani, H.; Amann, M.; Anderson, H.R.; Andrews, K.G.; Aryee, M.; et al. A comparative risk assessment of burden of disease and injury attributable to 67 risk factors and risk factor clusters in 21 regions, 1990–2010: A systematic analysis for the global burden of disease study 2010. *Lancet* **2012**, *380*, 2224–2260. [[CrossRef](#)]
- Lee, M.; Kloog, I.; Chudnovsky, A.; Lyapustin, A.; Wang, Y.; Melly, S.; Coull, B.; Koutrakis, P.; Schwartz, J. Spatiotemporal prediction of fine particulate matter using high-resolution satellite images in the southeastern U.S. 2003–2011. *J. Expo. Sci. Environ. Epidemiol.* **2016**, *26*, 377–384. [[CrossRef](#)] [[PubMed](#)]
- Sinha, P.R.; Gupta, P.; Kaskaoutis, D.G.; Sahu, L.K.; Nagendra, N.; Manchanda, R.K.; Kumar, Y.B.; Sreenivasan, S. Estimation of particulate matter from satellite- and ground-based observations over Hyderabad, India. *Int. J. Remote Sens.* **2015**, *36*, 6192–6213. [[CrossRef](#)]
- Mordukhovich, I.; Coull, B.; Kloog, I.; Koutrakis, P.; Vokonas, P.; Schwartz, J. Exposure to sub-chronic and long-term particulate air pollution and heart rate variability in an elderly cohort: The normative aging study. *Environ. Health* **2015**, *14*, 1–10. [[CrossRef](#)] [[PubMed](#)]

10. Liu, D.-J.; Li, L. Application study of comprehensive forecasting model based on entropy weighting method on trend of PM_{2.5} concentration in Guangzhou, China. *Int. J. Environ. Res. Public Health* **2015**, *12*, 7085–7099. [[CrossRef](#)] [[PubMed](#)]
11. Gupta, P.; Christopher, S.A. An evaluation of Terra-MODIS sampling for monthly and annual particulate matter air quality assessment over the southeastern United States. *Atmos. Environ.* **2008**, *42*, 6465–6471. [[CrossRef](#)]
12. Lee, M.; Koutrakis, P.; Coull, B.; Kloog, I.; Schwartz, J. Acute effect of fine particulate matter on mortality in three southeastern states from 2007–2011. *J. Expo. Sci. Environ. Epidemiol.* **2015**. [[CrossRef](#)] [[PubMed](#)]
13. Liu, Y.; Koutrakis, P.; Kahn, R. Estimating fine particulate matter component concentrations and size distributions using satellite-retrieved fractional aerosol optical depth: Part 2—A case study. *J. Air Waste Manag. Assoc.* **2007**, *57*, 1360–1369. [[PubMed](#)]
14. Zhang, Y.L.; Cao, F. Fine particulate matter (PM_{2.5}) in china at a city level. *Sci. Rep.* **2015**, *5*, 14884. [[CrossRef](#)] [[PubMed](#)]
15. Liu, Y. New directions: Satellite driven PM_{2.5} exposure models to support targeted particle pollution health effects research. *Atmos. Environ.* **2013**, *42*, 6465–6471. [[CrossRef](#)]
16. Wang, J. Intercomparison between satellite-derived aerosol optical thickness and PM_{2.5} mass: Implications for air quality studies. *Geophys. Res. Lett.* **2003**, *30*. [[CrossRef](#)]
17. Tao, J.; Zhang, M.; Chen, L.; Wang, Z.; Su, L.; Ge, C.; Han, X.; Zou, M. A method to estimate concentrations of surface-level particulate matter using satellite-based aerosol optical thickness. *Sci. China Earth Sci.* **2013**, *56*, 1422–1433. [[CrossRef](#)]
18. Liu, Y. Mapping annual mean ground-level PM_{2.5} concentrations using multiangle imaging spectroradiometer aerosol optical thickness over the contiguous United States. *J. Geophys. Res.* **2004**, *109*. [[CrossRef](#)]
19. Lee, H.J.; Liu, Y.; Coull, B.A.; Schwartz, J.; Koutrakis, P. A novel calibration approach of MODIS AOD data to predict PM_{2.5} concentrations. *Atmos. Chem. Phys. Discuss.* **2011**, *11*, 9769–9795. [[CrossRef](#)]
20. Liu, Y.; Franklin, M.; Kahn, R.; Koutrakis, P. Using aerosol optical thickness to predict ground-level PM_{2.5} concentrations in the St. Louis area: A comparison between MISR and MODIS. *Remote Sens. Environ.* **2007**, *107*, 33–44. [[CrossRef](#)]
21. Zhang, H.; Hoff, R.M.; Engel-Cox, J.A. The relation between moderate resolution imaging spectroradiometer (MODIS) aerosol optical depth and PM_{2.5} over the United States: A geographical comparison by U.S. Environmental Protection Agency regions. *J. Air Waste Manag. Assoc.* **2009**, *59*, 1358–1369. [[CrossRef](#)] [[PubMed](#)]
22. Liu, Y.; Koutrakis, P.; Kahn, R. Estimating fine particulate matter component concentrations and size distributions using satellite-retrieved fractional aerosol optical depth: Part 1—Method development. *J. Air Waste Manag. Assoc.* **2007**, *57*, 1351–1359. [[PubMed](#)]
23. Liu, Y.; Paciorek, C.J.; Koutrakis, P. Estimating regional spatial and temporal variability of PM_{2.5} concentrations using satellite data, meteorology, and land use information. *Environ. Health Perspect.* **2009**, *117*, 886–892. [[CrossRef](#)] [[PubMed](#)]
24. Paciorek, C.J.; Liu, Y.; Moreno-Macias, H.; Kondragunta, S. Spatiotemporal associations between goes aerosol optical depth retrievals and ground-level PM_{2.5}. *Environ. Sci. Technol.* **2008**, *42*, 5800–5806. [[CrossRef](#)] [[PubMed](#)]
25. Leon, J.-F.; Liousse, C.; Galy-Lacaux, C.; Doumbia, T.; Cachier, H. Monitoring of ambient fine particulate matter concentrations from space: application to European and African cities. *Proc. SPIE* **2010**, 78262A. [[CrossRef](#)]
26. Kacenelenbogen, M.; Leon, J.F.; Chiapello, I.; Tanre, D. Characterization of aerosol pollution events in France using ground-based and polder-2 satellite data. *Atmos. Chem. Phys.* **2006**, *6*, 4843–4849. [[CrossRef](#)]
27. Van Donkelaar, A.; Martin, R.V.; Brauer, M.; Boys, B.L. Use of satellite observations for long-term exposure assessment of global concentrations of fine particulate matter. *Environ. Health Perspect.* **2015**, *123*, 135–143. [[CrossRef](#)] [[PubMed](#)]
28. Lary, D.J.; Faruque, F.S.; Malakar, N.; Moore, A.; Roscoe, B.; Adams, Z.L.; Eggleston, Y. Estimating the global abundance of ground level presence of particulate matter (PM_{2.5}). *Geosp. Health* **2014**, *7*, S611–S630. [[CrossRef](#)] [[PubMed](#)]

29. Li, J.; Carlson, B.E.; Laci, A.A. How well do satellite AOD observations represent the spatial and temporal variability of PM_{2.5} concentration for the United States? *Atmos. Environ.* **2015**, *102*, 260–273. [[CrossRef](#)]
30. Toth, T.D.; Zhang, J.; Campbell, J.R.; Hyer, E.J.; Reid, J.S.; Westphal, D.L. Impact of data quality and surface-to-column representativeness on the PM_{2.5}/satellite AOD relationship for the contiguous United States. *Atmos. Chem. Phys. Discuss.* **2014**, *14*, 6049–6062. [[CrossRef](#)]
31. Engel-Cox, J.A.; Holloman, C.H.; Coutant, B.W.; Hoff, R.M. Qualitative and quantitative evaluation of MODIS satellite sensor data for regional and urban scale air quality. *Atmos. Environ.* **2004**, *38*, 2495–2509. [[CrossRef](#)]
32. Hu, Z. Spatial analysis of MODIS aerosol optical depth, PM_{2.5}, and chronic coronary heart disease. *Int. J. Health Geogr.* **2009**, *8*, 27. [[CrossRef](#)] [[PubMed](#)]
33. Kloog, I.; Koutrakis, P.; Coull, B.A.; Lee, H.J.; Schwartz, J. Assessing temporally and spatially resolved PM_{2.5} exposures for epidemiological studies using satellite aerosol optical depth measurements. *Atmos. Environ.* **2011**, *45*, 6267–6275. [[CrossRef](#)]
34. Kloog, I.; Nordio, F.; Coull, B.A.; Schwartz, J. Incorporating local land use regression and satellite aerosol optical depth in a hybrid model of spatiotemporal PM_{2.5} exposures in the mid-atlantic states. *Environ. Sci. Technol.* **2012**, *46*, 11913–11921. [[CrossRef](#)] [[PubMed](#)]
35. Chudnovsky, A.A.; Lee, H.J.; Kostinski, A.; Kotlov, T.; Koutrakis, P. Prediction of daily fine particulate matter concentrations using aerosol optical depth retrievals from the Geostationary Operational Environmental Satellite (GOES). *J. Air Waste Manag. Assoc.* **2012**, *62*, 1022–1031. [[CrossRef](#)] [[PubMed](#)]
36. Higgs, G.; Sterling, D.A.; Aryal, S.; Vemulapalli, A.; Priftis, K.N.; Sifakis, N.I. Aerosol optical depth as a measure of particulate exposure using imputed censored data, and relationship with childhood asthma hospital admissions for 2004 in Athens, Greece. *Environ. Health Insights* **2015**, *9*, 27–33. [[CrossRef](#)] [[PubMed](#)]
37. Hutchison, K.D.; Smith, S.; Faruqui, S.J. Correlating MODIS aerosol optical thickness data with ground-based PM_{2.5} observations across Texas for use in a real-time air quality prediction system. *Atmos. Environ.* **2005**, *39*, 7190–7203. [[CrossRef](#)]
38. Liu, Y.; Sarnat, J.A.; Kilaru, V.; Jacob, D.J.; Koutrakis, P. Estimating ground-level PM_{2.5} in the eastern United States using satellite remote sensing. *Environ. Sci. Technol.* **2005**, *39*, 3269–3278. [[CrossRef](#)] [[PubMed](#)]
39. Chu, D.A. Analysis of the relationship between MODIS aerosol optical depth and PM_{2.5} in the summertime US. *Proc. SPIE* **2006**, *6299*, 629903.
40. Engel-Cox, J.A.; Hoff, R.M.; Rogers, R.; Dimmick, F.; Rush, A.C.; Szykman, J.J.; Al-Saadi, J.; Chu, D.A.; Zell, E.R. Integrating lidar and satellite optical depth with ambient monitoring for 3-dimensional particulate characterization. *Atmos. Environ.* **2006**, *40*, 8056–8067. [[CrossRef](#)]
41. Gupta, P.; Christopher, S.A.; Wang, J.; Gehrig, R.; Lee, Y.; Kumar, N. Satellite remote sensing of particulate matter and air quality assessment over global cities. *Atmos. Environ.* **2006**, *40*, 5880–5892. [[CrossRef](#)]
42. Koelemeijer, R.B.A.; Homan, C.D.; Matthijsen, J. Comparison of spatial and temporal variations of aerosol optical thickness and particulate matter over Europe. *Atmos. Environ.* **2006**, *40*, 5304–5315. [[CrossRef](#)]
43. Van Donkelaar, A.; Martin, R.V.; Park, R.J. Estimating ground-level PM_{2.5} using aerosol optical depth determined from satellite remote sensing. *J. Geophys. Res.* **2006**, *111*. [[CrossRef](#)]
44. Kumar, N.; Chu, A.; Foster, A. An empirical relationship between PM_{2.5} and aerosol optical depth in Delhi metropolitan. *Atmos. Environ.* **2007**, *41*, 4492–4503. [[CrossRef](#)] [[PubMed](#)]
45. Wallace, J.; Kanaroglou, P. An investigation of air pollution in southern Ontario, Canada, with MODIS and MISR aerosol data. *Int. Geosci. Remote Sens.* **2007**, 4311–4314.
46. Gupta, P.; Christopher, S.A. Seven year particulate matter air quality assessment from surface and satellite measurements. *Atmos. Chem. Phys.* **2008**, *8*, 3311–3324. [[CrossRef](#)]
47. Hutchison, K.D.; Faruqui, S.J.; Smith, S. Improving correlations between MODIS aerosol optical thickness and ground-based PM_{2.5} observations through 3D spatial analyses. *Atmos. Environ.* **2008**, *42*, 530–543. [[CrossRef](#)]
48. Kumar, N.; Chu, A.; Foster, A. Remote sensing of ambient particles in Delhi and its environs: Estimation and validation. *Int. J. Remote Sens.* **2008**, *29*, 3383–3405. [[CrossRef](#)] [[PubMed](#)]
49. Al-Hamdan, M.Z.; Crosson, W.L.; Limaye, A.S.; Rickman, D.L.; Quattrochi, D.A.; Estes, M.G.; Qualters, J.R.; Sinclair, A.H.; Tolsma, D.D.; Adeniyi, K.A.; et al. Methods for characterizing fine particulate matter using ground observations and remotely sensed data: Potential use for environmental public health surveillance. *J. Air Waste Manag. Assoc.* **2009**, *59*, 865–881. [[CrossRef](#)] [[PubMed](#)]

50. Green, M.; Kondragunta, S.; Ciren, P.; Xu, C. Comparison of GEOS and MODIS aerosol optical depth (AOD) to aerosol robotic network (AERONET) AOD and improve PM_{2.5} mass at Bondville, Illinois. *J. Air Waste Manag. Assoc.* **2009**, *59*, 1082–1091. [[CrossRef](#)] [[PubMed](#)]
51. Gupta, P.; Christopher, S.A. Particulate matter air quality assessment using integrated surface, satellite, and meteorological products: Multiple regression approach. *J. Geophys. Res.* **2009**, *114*. [[CrossRef](#)]
52. Gupta, P.; Christopher, S.A. Particulate matter air quality assessment using integrated surface, satellite, and meteorological products: 2. A neural network approach. *J. Geophys. Res.* **2009**, *114*. [[CrossRef](#)]
53. Paciorek, C.J.; Liu, Y. Limitations of remotely sensed aerosol as a spatial proxy for fine particulate matter. *Environ. Health Perspect.* **2009**, *117*, 904–909. [[CrossRef](#)] [[PubMed](#)]
54. Schaap, M.; Apituley, A.; Timmermans, R.M.A.; Koelemeijer, R.B.A.; de Leeuw, G. Exploring the relation between aerosol optical depth and PM_{2.5} at Cabauw, The Netherlands. *Atmos. Chem. Phys.* **2009**, *9*, 909–925. [[CrossRef](#)]
55. Di Nicolantonio, W.; Cacciari, A. Modis multiannual observations in support of air quality monitoring in northern Italy. *Ital. J. Remote Sens. Riv. Ital. Telerilevamento* **2010**, *43*, 97–109.
56. Tian, J.; Chen, D. A semi-empirical model for predicting hourly ground-level fine particulate matter (PM_{2.5}) concentration in southern Ontario from satellite remote sensing and ground-based meteorological measurements. *Remote Sens. Environ.* **2010**, *114*, 221–229. [[CrossRef](#)]
57. Van Donkelaar, A.; Martin, R.V.; Brauer, M.; Kahn, R.; Levy, R.; Verduzco, C.; Villeneuve, P.J. Global estimates of ambient fine particulate matter concentrations from satellite-based aerosol optical depth: Development and application. *Environ. Health Perspect.* **2010**, *118*, 847–855. [[CrossRef](#)] [[PubMed](#)]
58. Wang, Z.; Chen, L.; Tao, J.; Zhang, Y.; Su, L. Satellite-based estimation of regional particulate matter (PM) in Beijing using vertical-and-RH correcting method. *Remote Sens. Environ.* **2010**, *114*, 50–63. [[CrossRef](#)]
59. Hu, Z.; Liebens, J.; Rao, K.R. Merging satellite measurement with ground-based air quality monitoring data to assess health effects of fine particulate matter pollution. In *Geospatial Analysis of Environmental Health*; Maantay, J.A., McLafferty, S., Eds.; Springer: Dordrecht, The Netherlands, 2011; Volume 4, pp. 395–409.
60. Hystad, P.; Setton, E.; Cervantes, A.; Poplawski, K.; Deschenes, S.; Brauer, M.; van Donkelaar, A.; Lamsal, L.; Martin, R.; Jerrett, M.; et al. Creating national air pollution models for population exposure assessment in Canada. *Environ. Health Perspect.* **2011**, *119*, 1123–1129. [[CrossRef](#)] [[PubMed](#)]
61. Wu, Y.; Guo, J.; Zhang, X.; Li, X. Correlation between PM concentrations and aerosol optical depth in eastern China based on BP neural networks. In Proceedings of the 2011 IEEE International Geoscience and Remote Sensing Symposium (IGRASS), Vancouver, BC, Canada, 24–29 July 2011.
62. Hystad, P.; Demers, P.A.; Johnson, K.C.; Brook, J.; van Donkelaar, A.; Lamsal, L.; Martin, R.; Brauer, M. Spatiotemporal air pollution exposure assessment for a Canadian population-based lung cancer case-control study. *Environ. Health* **2012**, *11*, 22. [[CrossRef](#)] [[PubMed](#)]
63. Lee, S.J.; Serre, M.L.; van Donkelaar, A.; Martin, R.V.; Burnett, R.T.; Jerrett, M. Comparison of geostatistical interpolation and remote sensing techniques for estimating long-term exposure to ambient PM_{2.5} concentrations across the continental United States. *Environ. Health Perspect.* **2012**, *120*, 1727–1732. [[CrossRef](#)] [[PubMed](#)]
64. Lee, H.J.; Coull, B.A.; Bell, M.L.; Koutrakis, P. Use of satellite-based aerosol optical depth and spatial clustering to predict ambient PM_{2.5} concentrations. *Environ. Res.* **2012**, *118*, 8–15. [[CrossRef](#)] [[PubMed](#)]
65. Liu, Y.; He, K.; Li, S.; Wang, Z.; Christiani, D.C.; Koutrakis, P. A statistical model to evaluate the effectiveness of PM_{2.5} emissions control during the Beijing 2008 Olympic Games. *Environ. Int.* **2012**, *44*, 100–105. [[CrossRef](#)] [[PubMed](#)]
66. Mao, L.; Qiu, Y.; Kusano, C.; Xu, X. Predicting regional space-time variation of PM_{2.5} with land-use regression model and MODIS data. *Environ. Sci. Pollut. Res. Int.* **2012**, *19*, 128–138. [[CrossRef](#)] [[PubMed](#)]
67. Van Donkelaar, A.; Martin, R.V.; Pasch, A.N.; Szykman, J.J.; Zhang, L.; Wang, Y.X.; Chen, D. Improving the accuracy of daily satellite-derived ground-level fine aerosol concentration estimates for north America. *Environ. Sci. Technol.* **2012**, *46*, 11971–11978. [[CrossRef](#)] [[PubMed](#)]
68. Wu, Y.; Guo, J.; Zhang, X.; Tian, X.; Zhang, J.; Wang, Y.; Duan, J.; Li, X. Synergy of satellite and ground based observations in estimation of particulate matter in eastern China. *Sci. Total Environ.* **2012**, *433*, 20–30. [[CrossRef](#)] [[PubMed](#)]

69. Beckerman, B.S.; Jerrett, M.; Martin, R.V.; van Donkelaar, A.; Ross, Z.; Burnett, R.T. Application of the deletion/substitution/addition algorithm to selecting land use regression models for interpolating air pollution measurements in California. *Atmos. Environ.* **2013**, *77*, 172–177. [[CrossRef](#)]
70. Beckerman, B.S.; Jerrett, M.; Serre, M.; Martin, R.V.; Lee, S.J.; van Donkelaar, A.; Ross, Z.; Su, J.; Burnett, R.T. A hybrid approach to estimating national scale spatiotemporal variability of PM_{2.5} in the contiguous United States. *Environ. Sci. Technol.* **2013**, *47*, 7233–7241. [[PubMed](#)]
71. Chudnovsky, A.A.; Kostinski, A.; Lyapustin, A.; Koutrakis, P. Spatial scales of pollution from variable resolution satellite imaging. *Environ. Pollut.* **2013**, *172*, 131–138. [[CrossRef](#)] [[PubMed](#)]
72. Chudnovsky, A.; Lyapustin, A.; Wang, Y.; Schwartz, J.; Koutrakis, P. Analyses of high resolution aerosol data from MODIS satellite: A MAIAC retrieval, southern New England, US. *Proc. SPIE* **2013**, *8795*, 8795E-1.
73. Cordero, L.; Wu, Y.; Gross, B.M.; Moshary, F. Assessing satellite AOD based and ARF/CMAQ output PM_{2.5} estimators. *Proc. SPIE* **2013**, *8723*, 872319.
74. Hu, X.; Waller, L.A.; Al-Hamdan, M.Z.; Crosson, W.L.; Estes, M.G., Jr.; Estes, S.M.; Quattrochi, D.A.; Sarnat, J.A.; Liu, Y. Estimating ground-level PM_{2.5} concentrations in the southeastern U.S. using geographically weighted regression. *Environ. Res.* **2013**, *121*, 1–10. [[CrossRef](#)] [[PubMed](#)]
75. Kumar, N.; Liang, D.; Comellas, A.; Chu, A.D.; Abrams, T. Satellite-based pm concentrations and their application to copd in Cleveland, OH. *J. Expo. Sci. Environ. Epidemiol.* **2013**, *23*, 637–646. [[CrossRef](#)] [[PubMed](#)]
76. Saunders, R.O.; Kahl, J.D.W.; Ghorai, J.K. Improved estimation of PM_{2.5} using lagrangian satellite-measured aerosol optical depth. *Atmos. Environ.* **2014**, *91*, 146–153. [[CrossRef](#)]
77. Strawa, A.W.; Chatfield, R.B.; Legg, M.; Scarnato, B.; Esswein, R. Improving retrievals of regional fine particulate matter concentrations from moderate resolution imaging spectroradiometer (MODIS) and ozone monitoring instrument (OMI) multisatellite observations. *J. Air Waste Manag. Assoc.* **2013**, *63*, 1434–1446. [[CrossRef](#)] [[PubMed](#)]
78. Chang, H.H.; Hu, X.; Liu, Y. Calibrating MODIS aerosol optical depth for predicting daily PM_{2.5} concentrations via statistical downscaling. *J. Expo. Sci. Environ. Epidemiol.* **2014**, *24*, 98–104. [[CrossRef](#)] [[PubMed](#)]
79. Chiu, Y.H.M.; Coull, B.A.; Sternthal, M.J.; Kloog, I.; Schwartz, J.; Cohen, S.; Wright, R.J. Effects of prenatal community violence and ambient air pollution on childhood wheeze in an urban population. *J. Allergy Clin. Immunol.* **2014**, *133*, 713–722 e714. [[CrossRef](#)] [[PubMed](#)]
80. Hu, X.; Waller, L.A.; Lyapustin, A.; Wang, Y.; Al-Hamdan, M.Z.; Crosson, W.L.; Estes, M.G.; Estes, S.M.; Quattrochi, D.A.; Puttaswamy, S.J.; et al. Estimating ground-level PM_{2.5} concentrations in the southeastern United States using maiaac AOD retrievals and a two-stage model. *Remote Sens. Environ.* **2014**, *140*, 220–232. [[CrossRef](#)]
81. Hu, X.; Waller, L.A.; Lyapustin, A.; Wang, Y.; Liu, Y. 10-year spatial and temporal trends of PM_{2.5} concentrations in the southeastern us estimated using high-resolution satellite data. *Atmos. Chem. Phys. Discuss.* **2014**, *14*, 6301–6314. [[CrossRef](#)]
82. Kloog, I.; Chudnovsky, A.A.; Just, A.C.; Nordio, F.; Koutrakis, P.; Coull, B.A.; Lyapustin, A.; Wang, Y.; Schwartz, J. A new hybrid spatio-temporal model for estimating daily multi-year PM_{2.5} concentrations across northeastern USA using high resolution aerosol optical depth data. *Atmos. Environ.* **2014**, *95*, 581–590. [[CrossRef](#)]
83. Kloog, I.; Nordio, F.; Zanobetti, A.; Coull, B.A.; Koutrakis, P.; Schwartz, J.D. Short term effects of particle exposure on hospital admissions in the Mid-Atlantic States: A population estimate. *PLoS ONE* **2014**, *9*, e88578. [[CrossRef](#)] [[PubMed](#)]
84. Kim, H.-S.; Chung, Y.-S.; Kim, J.-T. Spatio-temporal variations of optical properties of aerosols in East Asia measured by MODIS and relation to the ground-based mass concentrations observed in central Korea during 2001 similar to 2010. *Asia Pac. J. Atmos. Sci.* **2014**, *50*, 191–200. [[CrossRef](#)]
85. Lai, H.K.; Tsang, H.; Thach, T.Q.; Wong, C.M. Health impact assessment of exposure to fine particulate matter based on satellite and meteorological information. *Environ. Sci. Process Impacts* **2014**, *16*, 239–246. [[CrossRef](#)] [[PubMed](#)]
86. Lee, H.J.; Kang, C.M.; Coull, B.A.; Bell, M.L.; Koutrakis, P. Assessment of primary and secondary ambient particle trends using satellite aerosol optical depth and ground speciation data in the New England region, United States. *Environ. Res.* **2014**, *133*, 103–110. [[CrossRef](#)] [[PubMed](#)]

87. Ma, Z.; Hu, X.; Huang, L.; Bi, J.; Liu, Y. Estimating ground-level PM_{2.5} in China using satellite remote sensing. *Environ. Sci. Technol.* **2014**, *48*, 7436–7444. [[CrossRef](#)] [[PubMed](#)]
88. Rush, A.C.; Dougherty, J.J.; Engel-Cox, J.A. Correlating seasonal averaged in-situ monitoring of fine PM with satellite remote sensing data using geographic information system (GIS). *Proc. SPIE* **2014**, *5547*, 91–102.
89. Song, W.; Jia, H.; Huang, J.; Zhang, Y. A satellite-based geographically weighted regression model for regional PM_{2.5} estimation over the Pearl River Delta region in China. *Remote Sens. Environ.* **2014**, *154*, 1–7. [[CrossRef](#)]
90. Chan, S.H.; van Hee, V.C.; Bergen, S.; Szpiro, A.A.; DeRoo, L.A.; London, S.J.; Marshall, J.D.; Kaufman, J.D.; Sandler, D.P. Long-term air pollution exposure and blood pressure in the sister study. *Environ. Health Perspect.* **2015**, *123*, 951–958. [[CrossRef](#)] [[PubMed](#)]
91. Coker, E.; Ghosh, J.; Jerrett, M.; Gomez-Rubio, V.; Beckerman, B.; Cockburn, M.; Liverani, S.; Su, J.; Li, A.; Kile, M.L.; et al. Modeling spatial effects of PM_{2.5} on term low birth weight in Los Angeles county. *Environ. Res.* **2015**, *142*, 354–364. [[CrossRef](#)] [[PubMed](#)]
92. Geng, G.; Zhang, Q.; Martin, R.V.; van Donkelaar, A.; Huo, H.; Che, H.; Lin, J.; He, K. Estimating long-term PM_{2.5} concentrations in China using satellite-based aerosol optical depth and a chemical transport model. *Remote Sens. Environ.* **2015**, *166*, 262–270. [[CrossRef](#)]
93. Han, Y.; Wu, Y.; Wang, T.; Zhuang, B.; Li, S.; Zhao, K. Impacts of elevated-aerosol-layer and aerosol type on the correlation of AOD and particulate matter with ground-based and satellite measurements in Nanjing, southeast China. *Sci. Total Environ.* **2015**, *532*, 195–207. [[CrossRef](#)] [[PubMed](#)]
94. Just, A.C.; Wright, R.O.; Schwartz, J.; Coull, B.A.; Baccarelli, A.A.; Tellez-Rojo, M.M.; Moody, E.; Wang, Y.; Lyapustin, A.; Kloog, I. Using high-resolution satellite aerosol optical depth to estimate daily PM_{2.5} geographical distribution in Mexico City. *Environ. Sci. Technol.* **2015**, *49*, 8576–8584. [[CrossRef](#)] [[PubMed](#)]
95. Kloog, I.; Sorek-Hamer, M.; Lyapustin, A.; Coull, B.; Wang, Y.; Just, A.C.; Schwartz, J.; Broday, D.M. Estimating daily PM_{2.5} and PM₁₀ across the complex geo-climate region of Israel using maiaac satellite-based AOD data. *Atmos. Environ.* **2015**, *122*, 409–416. [[CrossRef](#)]
96. Leon Hsu, H.H.; Chiu, Y.H.M.; Coull, B.A.; Kloog, I.; Schwartz, J.; Lee, A.; Wright, R.O.; Wright, R.J. Prenatal particulate air pollution and asthma onset in urban children. Identifying sensitive windows and sex differences. *Am. J. Respir. Crit. Care Med.* **2015**, *192*, 1052–1059. [[CrossRef](#)] [[PubMed](#)]
97. Lin, C.; Li, Y.; Yuan, Z.; Lau, A.K.H.; Li, C.; Fung, J.C.H. Using satellite remote sensing data to estimate the high-resolution distribution of ground-level PM_{2.5}. *Remote Sens. Environ.* **2015**, *156*, 117–128. [[CrossRef](#)]
98. McHenry, J.N.; Vukovich, J.M.; Hsu, N.C. Development and implementation of a remote-sensing and in situ data-assimilating version of cmaq for operational PM_{2.5} forecasting. Part 1: Modis aerosol optical depth (AOD) data-assimilation design and testing. *J. Air Waste Manag. Assoc.* **2015**, *65*, 1395–1412. [[CrossRef](#)] [[PubMed](#)]
99. Nguyen, D.L.; Kim, J.Y.; Ghim, Y.S.; Shim, S.G. Influence of regional biomass burning on the highly elevated organic carbon concentrations observed at Gosan, South Korea during a strong asian dust period. *Environ. Sci. Pollut. Res. Int.* **2015**, *22*, 3594–3605. [[CrossRef](#)] [[PubMed](#)]
100. Song, Y.Z.; Yang, H.L.; Peng, J.H.; Song, Y.R.; Sun, Q.; Li, Y. Estimating PM_{2.5} concentrations in Xi'an city using a generalized additive model with multi-source monitoring data. *PLoS ONE* **2015**, *10*, e0142149. [[CrossRef](#)] [[PubMed](#)]
101. Van Donkelaar, A.; Martin, R.V.; Spurr, R.J.; Burnett, R.T. High-resolution satellite-derived PM_{2.5} from optimal estimation and geographically weighted regression over North America. *Environ. Sci. Technol.* **2015**, *49*, 10482–10491. [[CrossRef](#)] [[PubMed](#)]
102. Wong, C.M.; Lai, H.K.; Tsang, H.; Thach, T.Q.; Thomas, G.N.; Lam, K.B.; Chan, K.P.; Yang, L.; Lau, A.K.; Ayres, J.G.; et al. Satellite-based estimates of long-term exposure to fine particles and association with mortality in elderly Hong Kong residents. *Environ. Health Perspect.* **2015**, *123*, 1167–1172. [[CrossRef](#)] [[PubMed](#)]
103. Xie, Y.; Wang, Y.; Zhang, K.; Dong, W.; Lv, B.; Bai, Y. Daily estimation of ground-level PM_{2.5} concentrations over Beijing using 3 km resolution MODIS AOD. *Environ. Sci. Technol.* **2015**, *19*, 12280–12288. [[CrossRef](#)] [[PubMed](#)]
104. Xu, J.; Martin, R.V.; van Donkelaar, A.; Kim, J.; Choi, M.; Zhang, Q.; Geng, G.; Liu, Y.; Ma, Z.; Huang, L.; et al. Estimating ground-level PM_{2.5} in eastern china using aerosol optical depth determined from the goci satellite instrument. *Atmos. Chem. Phys. Discuss.* **2015**, *15*, 17251–17281. [[CrossRef](#)]

105. You, W.; Zang, Z.; Pan, X.; Zhang, L.; Chen, D. Estimating PM_{2.5} in Xi'an, china using aerosol optical depth: A comparison between the MODIS and MISR retrieval models. *Sci. Total Environ.* **2015**, *505*, 1156–1165. [[CrossRef](#)] [[PubMed](#)]
106. Zhang, Y.; Li, Z. Remote sensing of atmospheric fine particulate matter (PM_{2.5}) mass concentration near the ground from satellite observation. *Remote Sens. Environ.* **2015**, *160*, 252–262. [[CrossRef](#)]
107. Bai, Y.; Wu, L.; Qin, K.; Zhang, Y.; Shen, Y.; Zhou, Y. A geographically and temporally weighted regression model for ground-level PM_{2.5} estimation from satellite-derived 500 m resolution AOD. *Remote Sens.* **2016**, *8*, 262. [[CrossRef](#)]
108. Beloconi, A.; Kamarianakis, Y.; Chrysoulakis, N. Estimating urban PM₁₀ and PM_{2.5} concentrations, based on synergistic meris/aatsr aerosol observations, land cover and morphology data. *Remote Sens. Environ.* **2016**, *172*, 148–164. [[CrossRef](#)]
109. Crouse, D.L.; Philip, S.; van Donkelaar, A.; Martin, R.V.; Jessiman, B.; Peters, P.A.; Weichenthal, S.; Brook, J.R.; Hubbell, B.; Burnett, R.T. A new method to jointly estimate the mortality risk of long-term exposure to fine particulate matter and its components. *Sci. Rep.* **2016**, *6*, 18916. [[CrossRef](#)] [[PubMed](#)]
110. Di, Q.; Kloog, I.; Koutrakis, P.; Lyapustin, A.; Wang, Y.; Schwartz, J. Assessing PM_{2.5} exposures with high spatiotemporal resolution across the continental United States. *Environ. Sci. Technol.* **2016**, *50*, 4712–4721. [[CrossRef](#)] [[PubMed](#)]
111. Di, Q.; Koutrakis, P.; Schwartz, J. A hybrid prediction model for PM_{2.5} mass and components using a chemical transport model and land use regression. *Atmos. Environ.* **2016**, *131*, 390–399. [[CrossRef](#)]
112. Girguis, M.S.; Strickland, M.J.; Hu, X.; Liu, Y.; Bartell, S.M.; Vieira, V.M. Maternal exposure to traffic-related air pollution and birth defects in Massachusetts. *Environ. Res.* **2016**, *146*, 1–9. [[CrossRef](#)] [[PubMed](#)]
113. He, Q.; Zhou, G.; Geng, F.; Gao, W.; Yu, W. Spatial distribution of aerosol hygroscopicity and its effect on PM_{2.5} retrieval in east China. *Atmos. Res.* **2016**, *170*, 161–167. [[CrossRef](#)]
114. Kloog, I. Fine particulate matter (PM_{2.5}) association with peripheral artery disease admissions in northeastern United States. *Int. J. Environ. Health Res.* **2016**, *26*, 572–577. [[CrossRef](#)] [[PubMed](#)]
115. Karimian, H.; Li, Q.; Li, C.; Jin, L.; Fan, J.; Li, Y. An improved method for monitoring fine particulate matter mass concentrations via satellite remote sensing. *Aerosol Air Qual. Res.* **2016**, *16*, 1081–1092. [[CrossRef](#)]
116. Lee, H.J.; Chatfield, R.B.; Strawa, A.W. Enhancing the applicability of satellite remote sensing for PM_{2.5} estimation using MODIS deep blue AOD and land use regression in California, United States. *Environ. Sci. Technol.* **2016**, *50*, 6546–6555. [[CrossRef](#)] [[PubMed](#)]
117. Lin, C.; Li, Y.; Lau, A.K.H.; Deng, X.; Tse, T.K.T.; Fung, J.C.H.; Li, C.; Li, Z.; Lu, X.; Zhang, X.; et al. Estimation of long-term population exposure to PM_{2.5} for dense urban areas using 1-km MODIS data. *Remote Sens. Environ.* **2016**, *179*, 13–22. [[CrossRef](#)]
118. Lv, B.; Hu, Y.; Chang, H.H.; Russell, A.G.; Bai, Y. Improving the accuracy of daily PM_{2.5} distributions derived from the fusion of ground-level measurements with aerosol optical depth observations, a case study in north China. *Environ. Sci. Technol.* **2016**, *50*, 4752–4759. [[CrossRef](#)] [[PubMed](#)]
119. Ma, Z.; Hu, X.; Sayer, A.M.; Levy, R.; Zhang, Q.; Xue, Y.; Tong, S.; Bi, J.; Huang, L.; Liu, Y. Satellite-based spatiotemporal trends in PM_{2.5} concentrations: China, 2004–2013. *Environ. Health Perspect.* **2016**, *124*, 184–192. [[CrossRef](#)] [[PubMed](#)]
120. Shi, L.; Zanobetti, A.; Kloog, I.; Coull, B.A.; Koutrakis, P.; Melly, S.J.; Schwartz, J.D. Low-concentration pm and mortality: Estimating acute and chronic effects in a population-based study. *Environ. Health Perspect.* **2016**, *124*, 46–52. [[PubMed](#)]
121. Strickland, M.J.; Hao, H.; Hu, X.; Chang, H.H.; Darrow, L.A.; Liu, Y. Pediatric emergency visits and short-term changes in pm concentrations in the U.S. State of Georgia. *Environ. Health Perspect.* **2016**, *124*, 6900–6696.
122. Stieb, D.M.; Chen, L.; Beckerman, B.S.; Jerrett, M.; Crouse, D.L.; Omariba, D.W.; Peters, P.A.; van Donkelaar, A.; Martin, R.V.; Burnett, R.T.; et al. Associations of pregnancy outcomes and PM in a national Canadian study. *Environ. Health Perspect.* **2016**, *124*, 243–249. [[PubMed](#)]
123. Van Donkelaar, A.; Martin, R.V.; Brauer, M.; Hsu, N.C.; Kahn, R.A.; Levy, R.C.; Lyapustin, A.; Sayer, A.M.; Winker, D.M. Global estimates of fine particulate matter using a combined geophysical-statistical method with information from satellites, models, and monitors. *Environ. Sci. Technol.* **2016**, *50*, 3762–3772. [[CrossRef](#)] [[PubMed](#)]
124. Wang, B.; Chen, Z. High-resolution satellite-based analysis of ground-level PM_{2.5} for the city of Montreal. *Sci. Total Environ.* **2016**, *541*, 1059–1069. [[CrossRef](#)] [[PubMed](#)]

125. You, W.; Zang, Z.; Zhang, L.; Li, Y.; Pan, X.; Wang, W. National-scale estimates of ground-level PM_{2.5} concentration in china using geographically weighted regression based on 3 km resolution MODIS AOD. *Remote Sens.* **2016**, *8*, 184. [[CrossRef](#)]
126. You, W.; Zang, Z.; Zhang, L.; Li, Y.; Wang, W. Estimating national-scale ground-level PM_{2.5} concentration in china using geographically weighted regression based on MODIS and MISR AOD. *Environ. Sci. Pollut. Res. Int.* **2016**, *23*, 8327–8338. [[CrossRef](#)] [[PubMed](#)]
127. Zheng, Y.; Zhang, Q.; Liu, Y.; Geng, G.; He, K. Estimating ground-level PM_{2.5} concentrations over three megalopolises in china using satellite-derived aerosol optical depth measurements. *Atmos. Environ.* **2016**, *124*, 232–242. [[CrossRef](#)]
128. Zou, B. High-resolution satellite mapping of fine particulates based on geographically weighted regression. *IEEE Geosci. Remote Sens. Lett.* **2016**, *13*, 495–499. [[CrossRef](#)]
129. Guo, H.; Cheng, T.; Gu, X.; Gu, X.; Chen, H.; Wang, Y.; Zheng, F.; Xiang, K. Comparison of four ground-level PM_{2.5} estimation models using parasol aerosol optical depth data from China. *Int. J. Environ. Res. Public Health* **2016**, *13*, 180. [[CrossRef](#)] [[PubMed](#)]
130. Kloog, I.; Coull, B.A.; Zanobetti, A.; Koutrakis, P.; Schwartz, J.D. Acute and chronic effects of particles on hospital admissions in New-England. *PLoS ONE* **2012**, *7*, e34664. [[CrossRef](#)] [[PubMed](#)]
131. Kloog, I.; Ridgway, B.; Koutrakis, P.; Coull, B.A.; Schwartz, J.D. Long- and short-term exposure to PM_{2.5} and mortality: Using novel exposure models. *Epidemiology* **2013**, *24*, 555–561. [[CrossRef](#)] [[PubMed](#)]
132. Madrigano, J.; Kloog, I.; Goldberg, R.; Coull, B.A.; Mittleman, M.A.; Schwartz, J. Long-term exposure to PM_{2.5} and incidence of acute myocardial infarction. *Environ. Health Perspect.* **2013**, *121*, 192–196. [[PubMed](#)]
133. Lakshmanan, A.; hui, Y.H.; Coull, B.A.; Just, A.C.; Maxwell, S.L.; Schwartz, J.; Gryparis, A.; Kloog, I.; Wright, R.J.; Wright, R.O. Associations between prenatal traffic-related air pollution exposure and birth weight: Modification by sex and maternal pre-pregnancy body mass index. *Environ. Res.* **2015**, *137*, 268–277. [[CrossRef](#)] [[PubMed](#)]
134. Al-Hamdan, M.Z.; Crosson, W.L.; Economou, S.A.; Estes, M.G., Jr.; Estes, S.M.; Hemmings, S.N.; Kent, S.T.; Puckett, M.; Quattrochi, D.A.; Rickman, D.L.; et al. Environmental public health applications using remotely sensed data. *Geocarto Int.* **2014**, *29*, 85–98. [[CrossRef](#)] [[PubMed](#)]
135. Alexeeff, S.E.; Schwartz, J.; Kloog, I.; Chudnovsky, A.; Koutrakis, P.; Coull, B.A. Consequences of kriging and land use regression for PM_{2.5} predictions in epidemiologic analyses: Insights into spatial variability using high-resolution satellite data. *J. Expo. Sci. Environ. Epidemiol.* **2015**, *25*, 138–144. [[CrossRef](#)] [[PubMed](#)]
136. Ma, Z.; Liu, Y.; Zhao, Q.; Liu, M.; Zhou, Y.; Bi, J. Satellite-derived high resolution PM_{2.5} concentrations in yangtze river delta region of China using improved linear mixed effects model. *Atmos. Environ.* **2016**, *133*, 156–164. [[CrossRef](#)]
137. Kloog, I.; Melly, S.J.; Ridgway, W.L.; Coull, B.A.; Schwartz, J. Using new satellite based exposure methods to study the association between pregnancy PM_{2.5} exposure, premature birth and birth weight in massachusetts. *Environ. Health.* **2012**, *11*, 40. [[CrossRef](#)] [[PubMed](#)]
138. Liu, Y. Validation of multiangle imaging spectroradiometer (MISR) aerosol optical thickness measurements using aerosol robotic network (aeronet) observations over the contiguous United States. *J. Geophys. Res.* **2004**, *109*. [[CrossRef](#)]
139. Konkell, L. The view from afar satellite-derived estimates of global PM_{2.5}. *Environ. Health Perspect.* **2015**, *123*, A43. [[CrossRef](#)] [[PubMed](#)]
140. Spivey, A. Keeping an eye on PM_{2.5}: Satellite data reveal global picture of particulate pollution. *Environ. Health Perspect.* **2010**, *118*, A259. [[CrossRef](#)] [[PubMed](#)]
141. Crouse, D.L.; Peters, P.A.; van Donkelaar, A.; Goldberg, M.S.; Villeneuve, P.J.; Brion, O.; Khan, S.; Atari, D.O.; Jerrett, M.; Pope, C.A.; et al. Risk of non-accidental and cardiovascular mortality in relation to long-term exposure to low concentrations of fine particulate matter: A Canadian national-level cohort study. *Environ. Health Perspect.* **2012**, *120*, 708–714. [[CrossRef](#)] [[PubMed](#)]
142. Chen, B.; Sverdlik, L.; Imashev, S.; Solomon, P.; Lantz, J.; Schauer, J.; Shafer, M.; Artamonova, M.; Carmichael, G. Empirical relationship between particulate matter and aerosol optical depth over northern Tien-Shan, central Asia. *Air Qual. Atmos. Health.* **2013**, *6*, 385–396. [[CrossRef](#)]

143. Villeneuve, P.J.; Goldberg, M.S.; Burnett, R.T.; van Donkelaar, A.; Chen, H.; Martin, R.V. Associations between cigarette smoking, obesity, sociodemographic characteristics and remote-sensing-derived estimates of ambient PM_{2.5}: Results from a Canadian population-based survey. *Occup. Environ. Med.* **2011**, *68*, 920–927. [[CrossRef](#)] [[PubMed](#)]
144. To, T.; Zhu, J.; Villeneuve, P.J.; Simatovic, J.; Feldman, L.; Gao, C.; Williams, D.; Chen, H.; Weichenthal, S.; Wall, C.; et al. Chronic disease prevalence in women and air pollution—A 30-year longitudinal cohort study. *Environ. Int.* **2015**, *80*, 26–32. [[CrossRef](#)] [[PubMed](#)]
145. Brook, R.D.; Cakmak, S.; Turner, M.C.; Brook, J.R.; Crouse, D.L.; Peters, P.A.; van Donkelaar, A.; Villeneuve, P.J.; Brion, O.; Jerrett, M.; et al. Long-term fine particulate matter exposure and mortality from diabetes in Canada. *Diabetes Care* **2013**, *36*, 3313–3320. [[CrossRef](#)] [[PubMed](#)]
146. Jerrett, M.; Burnett, R.T.; Beckerman, B.S.; Turner, M.C.; Krewski, D.; Thurston, G.; Martin, R.V.; van Donkelaar, A.; Hughes, E.; Shi, Y.; et al. Spatial analysis of air pollution and mortality in California. *Am. J. Respir. Crit. Care Med.* **2013**, *188*, 593–599. [[CrossRef](#)] [[PubMed](#)]
147. Van Donkelaar, A.; Martin, R.V.; Spurr, R.J.D.; Drury, E.; Remer, L.A.; Levy, R.C.; Wang, J. Optimal estimation for global ground-level fine particulate matter concentrations. *J. Geophys. Res. Atmos.* **2013**, *118*, 5621–5636. [[CrossRef](#)]
148. Boys, B.L.; Martin, R.V.; van Donkelaar, A.; MacDonell, R.J.; Hsu, N.C.; Cooper, M.J.; Yantosca, R.M.; Lu, Z.; Streets, D.G.; Zhang, Q.; et al. Fifteen-year global time series of satellite-derived fine particulate matter. *Environ. Sci. Technol.* **2014**, *48*, 11109–11118. [[CrossRef](#)] [[PubMed](#)]
149. Lin, G.; Fu, J.; Jiang, D.; Hu, W.; Dong, D.; Huang, Y.; Zhao, M. Spatio-temporal variation of PM_{2.5} concentrations and their relationship with geographic and socioeconomic factors in China. *Int. J. Environ. Res. Public Health* **2014**, *11*, 173–186. [[CrossRef](#)] [[PubMed](#)]
150. Brauer, M.; Amann, M.; Burnett, R.T.; Cohen, A.; Dentener, F.; Ezzati, M.; Henderson, S.B.; Krzyzanowski, M.; Martin, R.V.; van Dingenen, R.; et al. Exposure assessment for estimation of the global burden of disease attributable to outdoor air pollution. *Environ. Sci. Technol.* **2012**, *46*, 652–660. [[CrossRef](#)] [[PubMed](#)]
151. Brunson, C.; Fotheringham, A.S.; Charlton, M.E. Geographically weighted regression: A method for exploring spatial nonstationarity. *Geogr. Anal.* **1996**, *28*, 281–298. [[CrossRef](#)]
152. Fotheringham, A.S.; Charlton, M.E.; Brunson, C. Geographically weighted regression: A natural evolution of the expansion method for spatial data analysis. *Environ. Plan. A* **1998**, *30*, 1905–1927. [[CrossRef](#)]
153. Fotheringham, A.S.; Brunson, C.; Charlton, M. Geographically weighted regression: The analysis of spatically varying relationships. In *Geographical Analysis*; O'Sullivan, D., Ed.; Wiley: New York, USA, 2003; Volume 35, pp. 272–275.



© 2016 by the authors; licensee MDPI, Basel, Switzerland. This article is an open access article distributed under the terms and conditions of the Creative Commons Attribution (CC-BY) license (<http://creativecommons.org/licenses/by/4.0/>).